UNIVERSIDADE FEDERAL DO PARANÁ

BRUNA CRISTINA BRÜLER

ULTRASSOM PERICÁRDIO-PULMONAR, ÂNGULO QRS-T FRONTAL E MECÂNICA MIOCÁRDICA: UM NOVO OLHAR PARA A DOENÇA MIXOMATOSA DA VALVA MITRAL.

CURITIBA
2022

BRUNA CRISTINA BRÜLER

ULTRASSOM PERICÁRDIO-PULMONAR, ÂNGULO QRS-T FRONTAL E MECÂNICA MIOCÁRDICA: UM NOVO OLHAR PARA A DOENÇA MIXOMATOSA DA VALVA MITRAL.

Tese apresentada ao Programa de Pós-graduação em Ciências Veterinárias, setor de Ciências Agrárias, Universidade Federal do Paraná, como requisito parcial à obtenção do título de doutor em Ciências Veterinárias.

Orientador: Prof. Dr. Marlos Gonçalves Sousa

CURITIBA

2022

DADOS INTERNACIONAIS DE CATALOGAÇÃO NA PUBLICAÇÃO (CIP)
UNIVERSIDADE FEDERAL DO PARANÁ
SISTEMA DE BIBLIOTECAS – BIBLIOTECA DE CIÊNCIAS AGRÁRIAS

Brüler, Bruna Cristina
Ultrasom pericárdio-pulmonar, ângulo QRS-T frontal e mecânica miocárdica: um novo olhar para a doença mixomatosa da valva mitral / Bruna Cristina Brüler . – Curitiba, 2022.
1 recurso online: PDF.

Tese (Doutorado) – Universidade Federal do Paraná, Setor de Ciências Agrárias, Programa de Pós-Graduação em Ciências Veterinárias.
Orientador: Prof. Dr. Marlos Gonçalves Sousa

1. Eletrocardiografia. 2. Ecocardiografia. 3. Arritmia. I. Sousa, Marlos Gonçalves. II. Universidade Federal do Paraná. Programa de Pós-Graduação em Ciências Veterinárias. III. Título.

Bibliotecária: Telma Terezinha Stresser de Assis CRB-9/944

MINISTÉRIO DA EDUCAÇÃO
SETOR DE CIÊNCIAS AGRÁRIAS
UNIVERSIDADE FEDERAL DO PARANÁ
PRÓ-REITORIA DE PESQUISA E PÓS-GRADUAÇÃO
PROGRAMA DE PÓS-GRADUAÇÃO CIÊNCIAS VETERINÁRIAS - 40001016023P3

TERMO DE APROVAÇÃO

Os membros da Banca Examinadora designada pelo Colegiado do Programa de Pós-Graduação CIÊNCIAS VETERINÁRIAS da Universidade Federal do Paraná foram convocados para realizar a arguição da tese de Doutorado de **BRUNA CRISTINA BRÜLER** intitulada: **Ultrassom pericárdio-pulmonar, ângulo QRS-T frontal e mecânica miocárdica: um novo olhar para a doença mixomatosa da valva mitral.**, sob orientação do Prof. Dr. MARLOS GONÇALVES SOUSA, que após terem inquirido a aluna e realizada a avaliação do trabalho, são de parecer pela sua APROVAÇÃO no rito de defesa.
A outorga do título de doutora está sujeita à homologação pelo colegiado, ao atendimento de todas as indicações e correções solicitadas pela banca e ao pleno atendimento das demandas regimentais do Programa de Pós-Graduação.

CURITIBA, 17 de Maio de 2022.

Assinatura Eletrônica
18/05/2022 08:33:18.0
MARLOS GONÇALVES SOUSA
Presidente da Banca Examinadora

Assinatura Eletrônica
18/05/2022 12:05:47.0
RUTHNÉA APARECIDA LÁZARO MUZZI
Avaliador Externo (UNIVERSIDADE FEDERAL DE LAVRAS)

Assinatura Eletrônica
22/07/2022 18:43:19.0
ROSÂNGELA DE OLIVEIRA ALVES CARVALHO
Avaliador Externo (UNIVERSIDADE FEDERAL DE GOIÁS)

Assinatura Eletrônica
18/05/2022 08:49:25.0
JUAN CARLOS DUQUE MORENO
Avaliador Interno (UNIVERSIDADE FEDERAL DO PARANÁ)

Assinatura Eletrônica
18/05/2022 09:13:23.0
ANA PAULA SARRAFF LOPES
Avaliador Externo (PONTIFÍCIA UNIVERSIDADE CATÓLICA DO PARANÁ)

Documento assinado eletronicamente de acordo com o disposto na legislação federal Decreto 8539 de 08 de outubro de 2015.
Gerado e autenticado pelo SIGA-UFPR, com a seguinte identificação única: 186809
Para autenticar este documento/assinatura, acesse https://www.prppg.ufpr.br/siga/visitante/autenticacaoassinaturas.jsp e insira o codigo 186809

AGRADECIMENTOS

A Deus, por tornar tudo possível.

Aos meus pais José Otávio e Siomara e ao irmão Rafael, pelo amor incondicional, raízes sólidas e referências extraordinárias.

Ao professor Marlos pela orientação, confiança e paciência, quando eu menos mereci e mais precisei. Aos membros da banca por aceitarem contribuir em um momento tão fundamental para meu crescimento, e a tantos professores do programa de pós-graduação da UFPR pela participação direta e indireta nesta jornada, de mestre para doutora.

À equipe do Laboratório de Cardiologia Comparada do Hospital Veterinário UFPR, pelo aprendizado, crescimento e companheirismo sem medida.

Aos amigos, novos e antigos, que não soltaram minha mão até aqui. E a todos que me acolheram nessa jornada, e que escolheram permanecer ao meu lado nos desafios que virão.

A todos, meu mais sincero OBRIGADA!

"Valeu a pena? Tudo vale a pena
Se a alma não é pequena.
Quem quer passar além do Bojador
Tem que passar além da dor.
Deus, ao mar, o perigo e o abismo deu,
Mas nele é que espelhou o céu."
— Fernando Pessoa

RESUMO

Para a elaboração desta tese, foram estudadas formas não convencionais de avaliação de pacientes com doença valvar mitral, com o objetivo de trazer novos conhecimentos que contribuam para o diagnóstico, acompanhamento clínico e prognóstico da doença cardíaca mais prevalente em animais domésticos. Para tanto, este trabalho foi subdividido em introdução e três capítulos distintos. Inicialmente, procurou-se esclarecer sobre a fisiopatologia da doença, com ênfase nos métodos convencionais de diagnóstico, acompanhamento e prognóstico. No primeiro capítulo, investigou-se sobre a aplicação de um novo método de avaliação pulmonar, a ser inserido no estudo ecocardiográfico convencional, com o intuito de diferenciar distrição respiratória cardiogênica e não-cardiogênica. Os resultados mostraram que a aplicação da nova técnica tem alta repetibilidade, e com potencial de distinção diagnóstica de até 100% em alguns cenários. O segundo capítulo foca no estudo do ângulo QRS-T frontal, uma variável eletrocardiográfica de distúrbio de repolarização, e no seu papel como um indicador de arritmogênese e progressão da insuficiência valvar mitral, a partir de traçados eletrocardiográficos convencionais. O estudo mostrou que existe correlação positiva entre a progressão da doença e o aumento do ângulo estudado, assim como a ocorrência de complexos prematuros, atriais e ventriculares. Os achados deste estudo reforçam a presença de distúrbios de repolarização na doença valvar mitral, e chamam a atenção para o potencial diagnóstico e prognóstico de índices que identificam precocemente estes distúrbios, a partir de batimentos sinusais. Finalmente, o terceiro capítulo foca na avaliação ecocardiográfica da mecânica miocárdica na doença valvar mitral, a partir do diagrama "bulls-eye", técnica de strain derivada do speckle tracking, com aplicação clínica promissora na medicina, mas ainda pouco explorada na cardiologia veterinária. Este estudo trouxe outro olhar para a avaliação da função sistólica, com potencial de identificação de disfunções regionais, focos de arritmogênese e prejuízos mecânicos que antecipam sua manifestação quando comparados à ecocardiografia convencional.

Palavras-chave: Eletrocardiografia. Ecocardiografia. Doença mitral. Ultrasom pulmonar. Arritmia.

ABSTRACT

For the elaboration of this thesis, unconventional methods for the evaluation of patients with mitral valve disease were studied, with the objective of bringing a new perspective that contributes to the diagnosis, clinical follow-up and prognosis of the most prevalent heart disease in domestic animals. For this purpose, this work was subdivided into an introduction and three different chapters. Initially, we sought to clarify the pathophysiology of the disease, with emphasis on conventional methods of diagnosis, follow-up and prognosis. In the first chapter, we proposed a new method of pulmonary evaluation, to be added in the conventional echocardiographic study, in order to differentiate between cardiogenic and non-cardiogenic dyspnea. The results showed that the application of this new technique has high repeatability, with differentiation power up to 100% in some scenarios. The second chapter focuses on the study of the frontal QRS-T angle, an electrocardiographic indicator of repolarization disorder, and its role as a predictor of arrhythmogenesis and progression of mitral valve disease, based on conventional electrocardiographic tracings. This study showed that there is a positive correlation between the progression of mitral valve disease and the increase in this angle, as well as the occurrence of premature atrial and ventricular complexes. The findings of this study reinforce the presence of repolarization disorders in mitral valve disease and draws attention to the diagnostic and prognostic potential of indices that identify these disorders, still on sinus beats. Finally, the third chapter focuses on the echocardiographic assessment of myocardial mechanics in mitral valve disease, using the “bulls-eye” diagram, a strain technique derived from speckel tracking, with promising clinical application in medicine, but still understudied in veterinary cardiology. This research shed a light to the assessment of systolic function, with the potential to identify regional dysfunctions, arrhythmogenesis foci and mechanical damage of early manifestation, when compared to conventional echocardiography.

Keywords: Electrocardiography. Echocardiography. Mitral valve disease. Lung ultrasound. Arrhythmias

LISTA DE ABREVIATURAS

ACVIM	- American College of Veterinary Internal Medicine
ANT	- Anterior segment
ANT-LAT	- Anterior lateral segment
ANT-SEPT	- Anterior septal segment
AP2	- Apical-2-chambers
AP3	- Apical-3-chambers
AP4	- Apical-4-chambers
AUC	- Area under the curve
CPE	- Cardiogenic pulmonary edema
CVHD	- Chronic valvular heart disease
ECG	- Electrocardiogram
EF%	- Ejection fraction
E/IVRT	- Peak velocity of E wave isovolumic relaxation time ratio
Emax	- Peak velocity of E wave of transmitral flow
fQRSTa	- Frontal QRST angle
FS%	- Fractional shortening
GLS	- Global longitudinal strain
INF	- Inferior segment
INF-SEPT	- Inferior lateral segment
INF-LAT	- Inferior lateral segment
IVRT	- Isovolumic relaxation time
LA/Ao	- Left atrium to aortic root ratio
LPA4C	- Left parasternal apical 4-chamber view

LUS	- Lung ultrasound
LVFP	- Left ventricular filling pressure
LVIDdn	- Normalized left ventricular internal diameter in diastole
MMVD	- Myxomatous mitral valve disease
PD	- Pulmonary disease
RM	- Remodeled
RM&CONG	- Remodeled and with congestion
RPL4C	- Right parasternal long axis 4-chamber view
RPSAo	- Right parasternal short axis at the level of aortic valve
RPSPM	- Right parasternal short axis at the level of papillary muscles
ROC	- Receiver operating characteristic
SD	- Standard deviation
Tpte	- T-wave peak-end interval
Tpte/QT	- Ratio of T-wave peak-end interval and QT interval
VA	- Ventricular arrhythmias
VPCs	- Ventricular premature complexes

SUMÁRIO

INTRODUÇÃO

A degeneração mixomatosa da valva mitral (DMVM) é a principal causa de regurgitação mitral em cães, e representa a cardiopatia adquirida mais comum nessa espécie (Keene et al, 2019). Ainda que se especule quanto à possíveis fatores desencadeadores, admite-se que seja essencialmente uma condição primária, sendo mais frequente em cães de pequeno a médio porte (Fox et al., 2012). A existência de raças particularmente predispostas, como o Cavalier King Charles Spaniel, Dachshund, Poodle miniatura e Schnauzer miniatura, corroboram a hipótese de um componente hereditário determinante (Meurs et al, 2018). Cães machos são cerca de 1,5 vezes mais afetados que fêmeas, além de apresentar início mais precoce e progressão mais rápida da doença (Borgarelli et al., 2004). É rara em cães jovens, no entanto, é capaz de atingir níveis de prevalência superiores a 90% em cães com mais de 10 anos (Borgarelli et al., 2010). A DMVM apresenta progressão variável, o que permite que nos deparemos com pacientes que se mantém assintomáticos por toda a vida, até cães que evoluem para óbito em poucos meses por insuficiência cardíaca congestiva (Borgarelli et al, 2008).

A DMVM é caracterizada por uma protrusão anormal das cúspides mitrais para o átrio esquerdo, resultante da deposição contínua de glicosaminoglicanos nos folhetos e cordas tendíneas (Fox, 2012). Em análise histológica, a DMVM transforma os folhetos valvares, originalmente finos e translúcidos, em estruturas espessadas e irregulares (Fox, 2012). Esse espessamento compromete a coaptação valvar durante a sístole, resultando em refluxo sanguíneo, do ventrículo para o átrio (Whitney, 1974). Esse sangue regurgitado causa diminuição do volume ejetado pelo ventrículo a cada sístole, minimizando a quantidade de sangue ejetado por minuto. Para evitar quedas significativas da pressão arterial, mecanismos compensatórios neuro-hormonais são ativados, e incluem aumento do tônus simpático e supressão parassimpática, ativação do sistema renina-angiotensina-aldosteronan e secreção de vasopressina. A ativação crônica destes mecanismos, em conjunto com as modificações estruturais, é determinante para a progressão da doença. (Borgarelli et al, 2008).

O desequilíbrio autonômico na DMVM resulta em um aumento sustentado da frequência cardíaca de repouso, encurtando o período diastólico e aumentando o consumo de oxigênio pelo miocárdio. Além disso, o aumento da resistência vascular periférica resulta em aumento da pós-carga, o que também aumenta o gasto energético cardíaco. (Ramírez et al, 2001). Por último, a insuficiência mitral avançada e a retenção hídrica induzem ao remodelamento cardíaco, que se caracteriza essencialmente por dilatação atrioventricular esquerda, hipertrofia miocárdica excêntrica e alterações na matriz intercelular (Bonagura e

Schober, 2009). Estes corações cronicamente afetados podem evoluir para a insuficiência cardíaca congestiva, caracterizada pelo aumento das pressões de enchimento ventricular, congestão venosa e acúmulo anormal de líquidos nos sistemas orgânicos (Ware, 2001). Além disso, o estiramento cardíaco, juntamente com o aumento da frequência cardíaca de repouso, pode atuar como substrato e gatilho para o desenvolvimento de arritmias cardíacas (Verheule et al., 2003).

A fisiopatogenia das arritmias nesses indivíduos ainda não está completamente elucidada. No entanto, Crosara et al. (2010), em um estudo que recrutou 36 cães com DMVM, concluiu que a presença de arritmias é um achado comum nesses pacientes, independentemente da condição clínica. Além disso, foi documentado que a dilatação atrial está diretamente relacionada à exacerbação de arritmias supraventriculares, e que arritmias ventriculares foram significativamente mais frequentes em cães com DMVM clínica. Finalmente, foi demonstrado que distúrbios do ritmo em animais DMVM raramente resultam em sinais clínicos, como fadiga ou síncope, o que leva ao subdiagnóstico. Porém, embora os sinais clínicos sejam incomuns, existe uma preocupação com a incidência de arritmias ventriculares devido ao risco aumentado de morte súbita e danos crônicos devido à diminuição do débito cardíaco (Crosara et al., 2010). Por este motivo, a compreensão dos eventos eletrofisiológicos subjacentes aos distúrbios do ritmo é de suma importância, podendo fornecer indicadores capazes de predizer a ocorrência de arritmias que elevam o risco de óbito em cães com DMVM avançada. O eletrocardiograma de superfície de seis a 12 derivações é o exame mais comumente utilizado para o diagnóstico de alterações elétricas cardíacas, permitindo a identificação da origem e classificação quanto à localização, frequência e critérios de malignidade (Santilli et al, 2018). Recentemente, no entanto, além de seu papel convencional no diagnóstico de distúrbios elétricos, a avaliação eletrocardiográfica na doença mitral tem sido estudada não somente na identificação e classificação das arritmias, mas também na identificação de indicadores de arritmogênese aumentada em ritmos ainda sinusais (Brüler et al, 2018; Vila et al, 2021).

Já o exame ecocardiográfico, além de ser o método padrão ouro para determinação do diagnóstico de DMVM, também fornece informações importantes referentes à progressão da doença, como grau de dilatação do átrio e ventrículo esquerdos, presença de disfunção sistólica e o diagnóstico de hipertensão pulmonar (Borgarelli et al, 2010). A DMVM, apesar de ser uma doença essencialmente do aparato valvar, pode levar à alterações como fibroses miocárdicas nos estágios mais avançados, culminando em disfunção sistólica. Estudos mostram que o encurtamento longitudinal das fibras miocárdicas é a primeira função a ser afetada, ainda em estágios subclínicos, levando a um aumento compensatório no

encurtamento radial, a fim de manter a fração de ejeção em nível normal. (Mizuguchil *et al*., 2008). Desta forma, a avaliação da função sistólica ventricular pela ecocardiografia convencional, essencialmente refletora do encurtamento radial, torna-se imprecisa. (Zois et al., 2012).

Em se tratando da avaliação da função sistólica, as técnicas derivadas do *speckle tracking* são bem conhecida na medicina, embora a literatura seja escassa na medicina veterinária (Buss et al., 2012). *Speckles* são marcadores naturais do tecido miocárdico, oriundos da reflexão do feixe de som, que podem ser rastreados durante os ciclos cardíacos, e refletirem informações sobre deformação. Entre as técnicas ecocardiográficas derivadas do *speckle tracking*, está o *bulls eye*, que reflete uma informação visual e quantitativa a respeito da função sistólica global, por meio do mapeamento do VE e sua disposição na forma de um alvo (Phelan et al, 2012). Diferentemente da avaliação *Doppler*, a identificação dos *speckles* é independente do ângulo de incidência do ultrassom, permitindo a avaliação da mecânica cardíaca em três planos espaciais (circunferencial, longitudinal e radial), além de não ser impactado pela movimentação translacional. A técnica do *bulls-eye*, além de permitir a identificação de regiões com déficit sistólico, também é capaz de identificar discinesia ventricular e deformações cardíacas anormais, ainda pré-clínicas (Liu et al, 2016). Esta técnica, que já apresenta aplicação clínica promissora em alguns cenários médicos, é ainda pouco aplicada na cardiologia veterinária (Phelan et al, 2012).

Devido à elevada incidência de valvopatia mitral na população canina, bem como sua taxa de progressão variável, justifica-se a constante busca por novos métodos diagnósticos, assim como de indicadores prognósticos e preditivos de eventos clínicos adversos. A melhora constante desses indicadores permite responder à dúvidas frequentes de tutores e clínicos quanto à tempo de sobrevida, e frequência ideal de acompanhamentos com mais precisão. Ademais, se tratando de um paciente que será anestesiado ou em situação de emergência, ter recursos como estes à mão é primordial. Nesta tese, estudamos a aplicação de uma nova técnica ecocardiográfica para identificação de descompensação cardiogênica, índices eletrocardiográficos potencialmente úteis à partir de traçados de ECG convencionais, e uma perspectiva diferente para a avaliação da função sistólica em diferentes estágios da doença mitral. Espera-se com esse trabalho fornecer recursos simples, reprodutíveis e com aplicabilidade clínica que melhorem a compreensão e manejo da cardiopatia mais prevalente em cães.

REFERÊNCIAS

ATKINS, C.; BONAGURA, J.; ETTINGER, S.; FOX, P.; GORDON, S.; HAGGSTROM, J.; HAMLIN, R.;KEENE, B.; LUIS-FUENTES, V.; STEPIEN, R. Guidelines for the diagnosis and treatment of canine chronic valvular heart disease. **Journal of Veterinary Internal Medicine**, v.23, n.6, p.1142-1150, 2009.

BONAGURA, J.D.; SCHOBER, K.E. Can ventricular function be assessed by echocardiography in chronic canine mitral valve disease? **Journal of Small Animal Practice**, v.50, supll.1, p.12-24, 2009.

BORGARELLI, M.; HAGGSTROM, J. Canine Degenerative myxomatous mitral valve disease: natural history, clinical presentation and therapy. **Vet Clin Small Anim** v.40, p.651–663, 2010

BORGARELLI, M., SAVARINO, P., CROSARA, S. Survival characteristics and prognostic variables of dogs with mitral regurgitation attributable to myxomatous valve disease. **Journal of Veterinary Internal Medicine** 22: 120–128, 2008

BORGARELLI, M.; ZINI, E.; D'AGNOLO, G.; et al. Comparison of primary mitral valve disease in German shepherd dogs and in small breeds. **Journal of Veterinary Cardiology.** v.6:27-34, 2004.

BUSS SJ, MERELES D, EMAMI M, KOROSOGLOU G, RIFFEL JH, BERTEL D, SCHONLAND SO, HEGENBART U, KATUS HA, HARDT SE. Rapid assessment of longitudinal systolic left ventricular function using speckle tracking of the mitral annulus. **Clinical Research in Cardiology** 2012;101:273e80.

BRÜLER, BC.; JOJIMA, FS.; DITTRICH, G.; GIANNICO, AT.; SOUSA, MG. QT instability, an indicator of augmented arrhythmo- genesis, increases with the progression of myxomatous mitral valve disease in dogs. **Journal of Veterinary Cardiology v**.66 p254-66, 2018.

CHEN, X.; TERESHCHENKO, L.G.; BERGER, R.D.; TRAYANOVA, N.A.; Arrhythmia Risk Stratification based on QT Interval Instability: An Intracardiac Electrocardiogram Study, **Heart Rhythm**, v.10, n.6, p.875–880, 2013

CROSARA, S.; BORGARELLI, M.; HAGGSTROM, J. Holter monitoring in 36 dogs with myxomatous mitral valve disease. **The Journal of the Australian Veterinary Association**, v. 88, n.10, p.386-391, 2010

FOX, PR. Pathology of myxomatous mitral valve disease in dog. **Journal of Veterinary Cardiology**, p.103-126, 2012

HAGGSTROM, J.; HOGLUNG, K.; BORGARELLI, M. An update on treatment and prognostic indicators in canine myxomatous mitral valve disease. **Journal of Small Animal Practice**, v.50 p.25-33, 2009

KEENE, BW.; ATKINS, CE.; BONAGURA, JD.; FOX ,PR.; HAÄGGSTROM, J.; FUENTES, VL.; OYAMA, MA.; RUSH, JE.; STEPIEN, R.; UECHI, M. ACVIM consensus guidelines for the diagnosis and treatment of myxomatous mitral valve disease in dogs. **Journal of Veterinary Internal Medicine** v. 33 p1127-40, 2019

LIU, L.;TUOS,ZHANGJ,ZUOL,LIUF,HAOL,SUNY,YANGL, SHAO H, QI W, ZHOU X, GE S. Reduction of left ventricular longitudinal global and segmental systolic functions in patients with hypertrophic cardiomyopathy: study of two- dimensional tissue motion annular displacement. **Exp Ther Med** 2014;7:1457e64.

MEURS, KM.; FRIEDENBERG, SG.; WILLIAMS, B, et al. Evaluation of genes associated with human myxomatous mitral valve disease in dogs with familial myxomatous mitral valve degeneration. **Vet J.** v.232 p.16-19, 2018.

MIZUGUCHI Y, OISHI Y, MIYOSHI H, IUCHI A, NAGASE N, OKI T. The functional role of longitudinal, circumferential and radial myocardial deformation for regulating the early impairment of left ventricular contraction and relaxation in patients with cardiovascular risk factors: a study with two-dimensional strain imaging. **Journal of the American Society of Echocardiography** 2008;21:1138e44.

PHELAN, D.; COLLIER, P.;THAVENDIRANATHAN, P; et al. Relative apical sparing of longitudinal strain using two-dimensional speckle-tracking echocardiography is both sensitive and specific for the diagnosis of cardiac amyloidosis. **Heart** v. 98 p1442-1448, 2012.

RAMÍREZ, E.Y.; PLALANCA, I. M. Manejo de la insuficiencia cardíaca congestiva In: BELENERIAN, G.C.; MUCHA, C.J; CAMACHO, A.A. **Afecciones cardiovasculares em pequeños animales**. 1. ed. Buenos Aires: Intermédica, 2001

SANTILLI, RA; (2018). Chapter 2: Principals of Electrocardiography. In Santilli, Ra.; Moïse, S.; Pariaut, R.; Perego, M, **Electrocardiography of the Dog and Cat** (2ª ed., pp. 21-65). Edra S.p.A..

VERHEULE, S.; WILSON, E.; EVERETT, T.; SHANBHAG, S.; GOLDEN, C.; OLGIN, J. Alterations in atrial electrophysiology and tissue structure in a canine model of chronic atrial dilatation due to mitral regurgitation. **Circulation**, v.107, p.2615-2622, 2003.

VILA, BC.; CAMACHO, AA,; SOUSA, MG. T-wave peak-end interval and ratio of T-wave peak-end and QT intervals: novel arrhythmogenic and survival markers for dogs with myxomatous mitral valve disease. **Journal of Veterinary Cardiology** v.35, 25-41, 2021

WARE, W. A. O exame cardiovascular. In: NELSON, R. W.; COUTO, C. G. (Ed.) **Medicina interna de pequenos animais**. 2. ed. Rio de Janeiro

WHITNEY, J.C. Observation on the effect of age in the severity of heart valve lesions in the dog. **Journal of Small Animal Practice**, v.15, n.8, p.511-522, 1974.

ZOIS, NE., TIDHOLM, A., NAGGA, KM., MOESGAARD, SG., RASMUSSEN, CE., HA ÄGGSTRROM, J.; PEDERSEN, HD.; ABLAD, B.; NILSEN, HY.; OLSEN, LH. Radial and longitudinal strain and strain rate assessed by speckle-tracking echocardiography in dogs with myxomatous mitral valve disease. **Journal of Veterinary Internal Medicine** v.26 1309-19, 2012.

CHAPTER 1 - Role of Echocardiographic Views Adapted for Lung Evaluation in Diagnosis of Cardiogenic Pulmonary Edema in Dogs[1]

[1] *Written in accordance with the guidelines of American Journal of Veterinary Researh, available in https://avmajournals.avma.org/page/AJVR-instructions-for-authors*

MSc. Bruna C. Brüler[a]

PhD. Amália T. Giannico[a]

MSc. Marcela Wolf[a]

PhD. Marlos G. Sousa[a]

[a] Laboratory of Comparative Cardiology, Department of Veterinary Medicine, Federal University of Paraná (UFPR),

Rua dos Funcionários, 1540, CEP 80035-050, Curitiba, Paraná, Brazil.

*Corresponding author: Bruna C. Brüler

bbruler@gmail.com

STRUCTURED ABSTRACT

Objective: To determine whether echocardiographic views adapted for lung evaluation may help identify the cause of dyspnea in dogs.

Animals: 45 chronic valvular heart disease (CVHD) dogs without evidence of lung pathology on radiographs, 15 CVHD dogs with cardiogenic pulmonary edema and 15 CVHD dogs with pulmonary disease.

Procedures: Loop recordings of pericardial-lung ultrasound were gathered during echocardiography. Four different adapted views were recorded for each dog. Chest X-rays were the reference standard for pulmonary edema and/or disease. Videos were classified based on the number of B lines as NEGATIVE (0, 1, 2 or 3) or POSITIVE (>3 or confluent). Accuracy compared to chest X-rays was calculated. Multivariate analyses were performed using echocardiographic variables that reflect increased left ventricular filling pressures to distinguish pulmonary edema from disease.

Results: A POSITIVE classification distinguished dogs with pulmonary edema or disease from subclinical CVHD dogs, in all four views. The best views were right parasternal short axis at papillary muscle level and long axis 4 chambers view, both with the same sensitivity (86.7%) and a specificity of 95.6% and 82.2%, respectively. Interobserver agreement test generated a kappa of 0.88 and 0.86 for these views, respectively. Multivariate analyses showed that adding cutoff values of Emax > 130 cm/s, E/IVRT > 2.5 or LA/Ao > 2.0 distinguished pulmonary edema from disease with 100% specificity.

Clinical Relevance: Echocardiographic views adapted for lung evaluation, in addition to standard echocardiographic parameters, may aide in identifying the cause of dyspnea in dogs.

INTRODUCTION

Dyspnea is a common cause of admittance in small animal practice, and thoracic radiography is currently considered to be the clinical standard for diagnosis.[1-3] However the demand for multiple recumbences and physical restrain may exacerbate respiratory distress

in unstable patients. In addition, thoracic x-rays are of unspecified accuracy, especially when it comes to combined heart and lung disease.[4] The use of bedside lung ultrasound (LUS) has been validated and gained acceptance in veterinary medicine over the past decade, and can be an alternative for identifying pulmonary and pleural space disease in settings where radiography is not readily feasible, particularly in patients in severe respiratory distress.[5-8] The LUS technique is standardly performed with a high frequency curvilinear US probe in multiple focal points of the thoracic wall, and is based on the concepts that ultrasound beams do not transmit through aerated lungs. Curiously, the identification of ultrasonographic artifacts is the fundamental principle of this technique, which involves the observation of horizontal A-lines with a glide sign (dry lung pattern) versus the observation of increased vertical B-lines, also knows as "lung-rockets" (wet lung pattern).[9] Thus, while A lines are the result of the reverberation of the pleura in healthy lungs, the presence of B lines primarily reflect the presence of increased extravascular lung water and interstitial-alveolar infiltrates.[8-11]

Although LUS is considered a reliable and useful tool for detecting cardiogenic pulmonary edema (CPE) in dogs, there is consistent overlapping with parenchymal pulmonary disease.[7] Therefore, heart size and function should be assessed in addition to LUS, to increase diagnostic accuracy.

Echocardiography is the gold-standard tool to identify and stage chronic valvular heart disease (CVHD).[3,12] Volume overload and increased left atrial size and left ventricular filling pressures are underlying conditions associated with the development of CPE, and may be suspected upon the visualization of acknowledged echocardiographic variables of cardiac remodeling and pulmonary congestion.[13-15] Morphologic and Doppler-derived parameters however, although useful in refining diagnosis, do not give precise information regarding pulmonary parenchyma. Thoracic radiographs can be performed, but may be challenging in patients with respiratory distress. Bedside LUS is generally safe in unstable patients, but gives no information regarding heart size and function, and has marked overlapping with pulmonary disease such as pneumonia.[7,8] An integrated approach evaluating the lungs, pleural space, and heart should lead to an improved accuracy of diagnosis. In this study the authors

hypothesized that additional information regarding pulmonary edema and/or disease could be obtained during standard echocardiography, limiting the need of multiple exams in challenging conditions. Therefore, the purposes of this study were (1) to test if sector transducers are useful in identifying wet lung patterns during echocardiographic examination, when focused on the pericardial-lung interface; (2) to identify the best adapted echocardiographic views for such purpose; and (3) to determine if the combination of cardiac remodeling, doppler-derived indices of elevated left ventricular filling pressures and wet lung pattern, obtained from echocardiography alone, may refine the diagnosis of the underlying cause of dyspnea in dogs.

MATERIALS AND METHODS

Dogs recruited for this prospective multicenter cross-sectional study were selected among patients admitted for veterinary care at a wide range of private veterinary clinics. All procedures received client consent and were previously approved by UFPR's institutional Animal Use Committee and complied with the National Institutes of Health Guide for the Care and Use of Laboratory Animals.

In order to be included in the study, the diagnosis and staging of CVHD in dogs was required, which was based on clinical history, echocardiographic identification of impaired valvar anatomy, presence or not of cardiac remodeling and clinical manifestation or absence of respiratory distress[3, 12, 16]. Dogs presenting with respiratory signs and with a medical history, physical examination and blood work indicative of primary pulmonary disease of multiple causes were also gathered to compose a pulmonary disease (PD) group. Dogs with another concomitant heart disease in addition to CVHD, or clinically debilitaded dogs due to other systemic underlying conditions were not enrolled in the study. For asymptomatic CVHD dogs with and without cardiac remodeling, and for dogs with CPE or PD, two-view thoracic radiography was used as the reference standard for pulmonary findings. Dogs that could not tolerate radiographic or echocardiographic examination within 3 hours of admittance were also excluded from the study. A diffuse distribution of interstitial to alveolar pulmonary infiltrates,

along with left cardiac enlargement and a positive clinical response to diuretic therapy was considered diagnostic of CPE.[17] Echocardiography was carried out by either one of two operators, with over 7 years of experience (BCB and ATG) using an ultrasonography system (MySono U6 – Samsung, Suwon, South Korea) equipped with 3.0-8.0 MHz and 2.0-4.0 MHz phased array transducers (P2-4 and P3-8 reference – Samsung, Suwon, South Korea).

During echocardiographic examination, loop recordings with increased depth, placement of the heart in the upper 1/3 of the screen and positioning of the focal point at the lung plane were used for image gathering and posterior post-acquisition evaluation in the following standard echocardiographic views: left parasternal apical 4-chamber view (LPA4C), right parasternal short axis at the level of aortic valve (RPSAo), right parasternal short axis at the level of papillary muscles (RPSPM) and right parasternal long axis 4-chamber view (RPL4C). A schematic figure of the adapted views, along with the corresponding echocardiographic images is shown in Figure 1. The videos were recorded immediately after routine evaluation of each window, not adding significant amount of time to the exam. Also, echocardiographic parameters including left atrium aortic root ratio (LA/Ao)[18], normalized left ventricular internal diameter in diastole (LVIDDn)[19], peak velocity of E wave of transmitral flow (Emax), isovolumic relaxation time (IVRT) and peak velocity of E wave isovolumic relaxation time ratio (E/IVRT) were either measured or calculated for each dog for the sorting of groups, and posterior statistical analyses. During the exam, dogs were placed in lateral recumbence and maintained in position by gentle physical restraint. Dogs considered too unstable to tolerate this maneuver were not admitted in the study.

For analyses and statistical purposes, dogs were divided into 5 different groups based on cardiac remodeling according to the American College of Veterinary Internal Medicine (ACVIM) classification scheme[3] (stage B defined as subclinical heart disease without (B1) or with (B2) evidence of left cardiomegaly, defined as both LA/Ao ≥ 1.6 and LVIDDn > 1.7), presence or absence of increased LV filling pressures and radiographic evidence of pulmonary edema or disease (interstitial and/or alveolar lung patterns)[3,20] . The groups were named as follows: 1) Control (CVHD stage B1 patients); 2) RM (CVHD stage B2 patients presenting low

evidence of increased left ventricular filling pressure (LVFP) (Emax < 1.0 m/s and E/IVRT < 2.0); 3) RM&CONG (CVHD stage B2 with strong evidence of increased LVFP and congestion of pulmonary veins (Emax > 1.3 m/s and E/IVRT > 2.5); 4): Cardiogenic pulmonary edema (CPE); and 5) Pulmonary disease (PD). For each dog, four video loops were obtained (LPA4C, RPSAo, RPSPM and RPL4C) for post-acquisition assessment. In each video, the number of B lines (hyper-echoic vertical lines extending without fading from the pericardial-lung interface to the far aspect of the ultrasound screen) was tabulated. The analyses were performed individually by 2 veterinary cardiologists, blinded to the dogs' clinical, echocardiographic, and radiographic data. The number of B lines was classified as 0, 1, 2, 3, >3 or confluent (too many to count), and each video was marked as NEGATIVE (0, 1, 2 or 3) or POSITIVE (>3 or confluent).

STATISTICAL ANALYSES

Statistical analyses were performed using commercially available software. All data underwent the Shapiro-Wilk normality test. Mean and standard deviation (SD) were used to provide descriptive statistics for normally distributed continuous variables. Data obtained from echocardiographic variables were compared. An analysis of variance followed by Tukey´s multiple comparison test was used to investigate differences between groups. To evaluate the accuracy of a POSITIVE/NEGATIVE classification in distinguishing CPE and PD from the other three groups, relative frequencies were estimated for these results, in each one of the four adapted views. The association between these classifications was checked with a chi-square test. Based on these frequencies, sensitivity, specificity, positive and negative predictive values, accuracy and the odds-ratio of each view were obtained. The level of agreement between two investigators was further examined by calculation of Cohen's kappa. Levels of agreement based on kappa values were interpreted as poor (0.00–0.20); mild (0.21–0.40); moderate (0.41–0.60); good (0.61–0.80); very good (0.81–1.00). Finally, multivariate analyses was performed, with predetermined cutoff values of Emax, LA/Ao and E/IVRT, to distinguish

POSITIVE CPE dogs from PD dogs. For all analyses, statistical significance was set at $P < 0.05$.

RESULTS

Seventy-five client-owned dogs that met all inclusion criteria among the total of animals recruited by the end of the study were enrolled. The age and body weight of the animals ranged from 6-16 years and 1.7-21.7 kg, respectively. There was no difference between groups regarding weight (P= 0.908), but a significant difference in age was documented between the control group and every other group (P<0.001). Several breeds were included, but mixed-bred (n=13, 17.3%), Miniature Poodles (n=10, 13.3%) and Lhasa apsos (n=10, 13.3%) were overrepresented. Descriptive statistics of the studied population is shown in Table 1.

Of the fifteen dogs with confirmed CPE, five (33.33%) were previously diagnosed stage C patients, in chronic use of pimobendan, furosemide, benazepril and spironolactone, whereas two (13.33%) were stage B2 dogs, in chronic use of pimobendan alone. The remaining eight (53,33%) dogs in CPE group had no previous diagnosis of cardiac disease, and were not taking any chronic medication.

Of the thirty dogs with remodeled hearts without CPE at the time of examination, nine (30%) were known stage B2 patients, in chronic use of pimobendan as monotherapy. The remaining 21 (70%) dogs had no previous history of cardiac disease, so no medication had been prescribed before.

Regarding the dogs in the respiratory group, twelve (46%) were diagnosed with pneumonia, five (33.3%) with chronic bronchitis, two (13.33%) were diagnosed with pulmonary metastasis, and one (6.66%) was diagnosed with neurogenic edema attributable to cluster seizures. None of the dogs were in chronic use of medication at the time of diagnosis.

When arranging together groups with the same expected results based on positive radiographic findings (CPE + PD), 25 out of 30 (83,33%), 23/30 (76,66%), 26/30 (86,66%) and 26/30 (86,66%) videos were correctly classified as POSITIVE for views LPA4C, RPSAo, RPPM and RPL4C, respectively. Similarly, with groups Control, RM and RM&CONG, 32 out

of 45 (71.11%), 28/45 (62.22%), 43/45 (95.55%) and 37/45 (82.22%) were correctly classified as NEGATIVE when using images LPA4C, RPSAo, RPAP and RPL4C, respectively (Figure 2).

A positive classification based on each of the four adapted echocardiographic views (>3 or confluent B lines) was able to differentiate dogs with cardiogenic edema or pulmonary disease from animals without radiographic pulmonary infiltrates. Sensitivity, specificity, positive and negative predictive values, accuracy and the odds ratio are show in Table 2. Best interobserver agreement was obtained when RPSP and RPL4C images were used (kappa 0.88 and 0.86, respectively). An illustrative image of how the B lines behave in all 4 adapted views between groups is shown in Figure 3.

LA/Ao, Emax and E/IVRT were the echocardiographic variables used in the multivariate analyses. Cut-off values of 1.6 and 2.0 for LA/Ao, 1.0 m/s and 1.3 m/s for Emax and 2.5 for E/IVRT were able to distinguish dogs with CPE from dogs with PD with 100% specificity, for animals that had > 3 B lines in views RPSPM and RPL4C. Values of sensitivity, specificity, positive and negative predictive values and accuracy are show in Table 3.

DISCUSSION

Differentiating causes of respiratory distress in dogs is challenging in clinical practice, especially if based solely on medical history and physical examination.[21] Unsurprisingly, the majority of diagnostic tests involve some degree of physical restrain and stress to the patient. In addition, most test results are not conclusive on their own, which can be time consuming and, for some clients, cost-prohibitive. This study assessed whether a single diagnostic tool might be enough for heart and lung evaluation during critical settings.

The results of this investigation show that echocardiographic views adapted for lung evaluation, in addition to standard echocardiographic findings, are a straightforward way of ruling in or out CPE as the cause of dyspnea in dogs. The technique consists of applying LUS techniques with sector transducers during conventional echocardiographic examination, and

analyzing the previously described wet/dry lung patterns on the pericardial-lung interface. Our study has shown that a POSITIVE classification usually matches the findings of interstitial to alveolar pulmonary infiltrates found in thoracic radiographs in dogs with CPE and lung disease, in every one of the four different views tested.

Even though the four different views were able to identify CPE and PD, RPL4C and RPSPM were the ones with best accuracies (92% and 84%, respectively) and less false positives. In contrast, LPA4C and RPSAo, were the adapted views with most false negatives, suggesting a higher number of artifacts arising from the cardiac base even in healthy individuals. In addition to having the highest sensitivity and specificity, RPSPM is considerably easy to obtain, even in patients in standing position, which may be more suitable for dogs in respiratory distress. Our findings are in accordance with a recently published study on pericardial-lung-ultrasound, which used a similar technique for the identification of CPE.[22]

Differentiating cardiac from non-cardiac causes of dyspnea has long been of interest in various studies, especially due to the urgency that such situations require.[23] The clinical utility of biomarkers such as natriuretic peptides has been previously reported, owing to their relation with cardiac stretch[24]. However, no test is optimal when used as a single modality approach, and the unavailability of a point-of-care canine NT-proBNP assay limits its utility in the emergency setting.[25]

Although LUS is well validated in dogs, with ≥ 3 B lines within a single intercostal space being a surrogate for CPE[8], such technique could not differentiate CPE from other causes of alveolar-interstitial syndrome, since parenchymal pulmonary diseases produce the same wet-lung pattern.[7,8] For this reason, information regarding underlying cardiac disease and staging is of utmost clinical importance. Although the auscultation of a systolic apical murmur during physical examination in small dogs over 6 years of age is highly suggestive of CVHD, an echocardiogram is fundamental to confirm and stage the disease, as well as identify increased left ventricular filling pressures.[12,14,15] Adding lung evaluation by means of the adapted RPSPM echocardiographic view proposed by the authors to a standard echocardiographic examination showed a high positive predictive value (92,9%) in the identification of wet lung pattern, in

addition to reliably informing about cardiac condition, solving the inconvenience of pulmonary disease overlapping.

The interobserver agreement was very good for views RPSPM and RPL4C (kappa 0.88 and 0.86, respectively), which makes this technique repeatable for cardiologists and intensivists in the clinical setting. The method of classification, as it is with standard LUS, is very straightforward and not time consuming, allowing for immediate diagnosis and therapeutic management. In cases where cardiogenic edema is ruled out by lack of cardiac enlargement, but pulmonary disease is suspected upon the visualization of >3 B lines, further diagnostic tools such as thoracic radiographs, bronchoscopy or computerized tomography scans should be considered.[26,27] Nonetheless, for patients in respiratory distress it seems enough for the immediate therapeutic management, especially when it comes to deciding upon the use of diuretics.

Although the technique discussed in this study is accurate in identifying wet-lung patterns, there was no way, as expected, to distinguish CPE from PD by the visualization of the B lines alone. For this reason, the authors recommend the technique to be used as an extension of the standard echocardiographic examination. In spite of doppler variables of increased left ventricular filling pressures demanding a higher degree of specialty, and being difficult to obtain from dogs in severe respiratory distress, LA/Ao performed well, and many studies have showed that non-specialists can obtain LA/Ao ratios consistently through focused echocardiograms in an acute care setting[28,29]. Multivariate analyses in this study showed that adding known cutoff values of LA/Ao can increase the specificity of the B lines in diagnosing CPE up to 100%.[14]

An important limitation of this research relates to the uncontrolled long-term medical treatment in patients in groups RM, RM&CONG and CPE. Nonetheless, positive classifications were still able to identify patients in CPE, as seen on thoracic radiographs. Another limitation is that the PD group is predominantly represented by pneumonia and chronic bronchitis (80%), which limits the extrapolation of these results to other pulmonary diseases, especially when it comes to focal pulmonary conditions. Furthermore, with the exception of a single patient where

pulmonary metastasis was an unexpected finding, most patients presented some degree of respiratory distress at the time of the exam, which also might limit the applicability of our findings to patients with incipient diseases and mild respiratory signs. Although there was no difference between groups regarding weight, the effect of body condition over lung artifacts should be taken into consideration. In addition, although statistical analyses showed values of specificity up to 100% for the cutoff values used, one must not forget that this is a reflection of the studied population, where no marked overlapping of advanced cardiac remodeling and pulmonary disease was documented. Thus, one must keep in mind that these conditions may coexist as comorbidities, which may impact the accuracy of this technique when used in the clinical setting. It also should be pointed out that, although this study was directed to a population of CVHD dogs, there is no reason to believe this technique cannot be extrapolated to dogs or cats due to other clinical heart diseases. Future studies should be conducted in order to warrant this statement. Finally, the authors do not advise against the use multiple diagnostic techniques. However, pericardial-LUS, in addition to conventional echocardiographic exam, is appropriate for fast clinical decision-making, leading to an effective approach during the first critical hours of treatment.

CONCLUSIONS

This research showed that sectorial transducers are efficient in the detection of wet lung patterns, with RPSPM and RPL4C performing as the most precise and repeatable adapted echocardiographic views. When used alone, pericardial LUS was not able to accurately differentiate CPE and PD. However, when combined with echocardiographic variables of cardiac remodeling and increased left ventricular filling pressures, it was highly sensitive and specific for confirming CPE as the cause of respiratory distress. Adapting standard views for lung evaluation during echocardiography in dogs sufficiently stable to handle this exam is a simple, reliable, repeatable, and time sparing ancillary technique, that aides in the diagnosis of respiratory distress in dogs.

REFERENCES

1. Rozanski E, Chan D. Approach to the patient with respiratory distress. *Vet Clin North Am Small Anim Pract.* 2005;35(2):307- 317.

2. Dear JD. Bacterial Pneumonia in Dogs and Cats: An Update. *Vet Clin North Am Small Anim Pract.* 2020;50(2):447- 465.

3. Atkins C, Bonagura J, Ettinger S, et al. Guidelines for the diagnosis and treatment of canine chronic valvular heart disease. *J Vet Intern Med*. 2009;23(6):1142 -1150.

4. Balbarini A, Limbruno U, Bertoli D, et al. Evaluation of pulmonary vascular pressures in cardiac patients: The role of the chest roentgenogram. *J Thorac Imaging.* 1991;6:62 – 68.

5. Rademacher N, Pariaut R, Pate J, et al. Transthoracic lung ultrasound in normal dogs and dogs with cardiogenic pulmonary edema: A pilot study. *Vet Radiol Ultrasound.* 2014; 55:447–452.

6. Lisciandro GR, Fulton RM, Fosgate GT, et al. Frequency of B-lines using a regionally-based lung ultrasound examination in cats with normal thoracic radiographically normal lungs compared with left- sided congestive heart failure. *J Vet Emerg Crit Care* 2017; 27(5): 499 – 505.

7. Ward JL, Lisciandro GR, Keene BW, et al. Accuracy of point-of-care lung ultrasonography for the diagnosis of cardiogenic pulmonary edema in dogs and cats with acute dyspnea. *J Am Vet Med Assoc*. 2017;250:666-675.

8. Lisciandro GR, Fosgate GT, Fulton RM. Frequency and number of ultrasound lung rockets (B-lines) using a regionally based lung ultra- sound examination named vet BLUE (veterinary bedside lung ultra- sound exam) in dogs with radiographically normal lung findings. *Vet Radiol Ultrasound* 2014;55:315 - 322.

9. Baad M, Lu ZF, Reiser I, et al. Clinical significance of US artifacts. *Radiographics* 2017;37:1408 –1423.

10. Lichtenstein D, Meziere G, Biderman P, et al. The comet-tail artifact. An ultrasound sign of

alveolar-interstitial syndrome. *Am J Respir Crit Care Med* 1997;156:1640 – 1646.

11. Louvet A, Bourgeois JM. Lung ring-down artifact as a sign of pulmonary alveolar-interstitial disease. *Vet Radiol Ultrasound* 2008;49:374 – 377.

12. Chetboul V, Tissier R. Echocardiographic assessment of canine degenerative mitral valve disease. *J Vet Cardio*. 2012;14:127 - 148.

13 Ohno M, Cheng CP, Little WC. Mechanism of altered patterns of left ventricular filling during the development of congestive heart failure. *Circulation* 1994;89:2241 – 2250.

14. Schober KE, Bonagura JD, Scansen BA, et al. Estimation of left ventricular filling pressure by use of Doppler echocardiography in healthy anesthetized dogs subjected to acute volume loading. *Am J Vet Res* 2008:69;1034 – 1049.

15. Schober KE, Hart TM, Stern JA, et al. Detection of congestive heart failure in dogs by Doppler echocardiography. *J Vet Intern Med* 2010;24:1358 - 1368.

16. Borgarelli M, Haggstrom J. Canine Degenerative myxomatous mitral valve disease: natural history, clinical presentation and therapy. *Vet Clin Small Anim* 2010;40:651 – 663.

17. Diana A, Guglielmini C, Pivetta M, et al. Radiographic features of cardiogenic pulmonary edema in dogs with mitral regurgitation: 61 cases (1998–2007). *J Am Vet Med Assoc* 2009;235:1058 – 1063.

18. Hansson K, Haggstrom J, Kvart C, Lord P. Left atrial to aortic root indices using two-dimensional and M-mode echocardiography in cavalier King Charles spaniels with and without left atrial enlargement. *Vet Radiol Ultrasound*. 2002;43(6):568 - 575.

19. Cornell CC, Kittleson MD, Della Torre P, et al. Allometric scaling of M-mode cardiac measurements in normal adult dogs. *J Vet Intern Med* 2004;18:311 – 321.

20. Ward JL, Lisciandro GR, DeFrancesco TC. Distribution of alveolar-interstitial syndrome in dogs and cats with respiratory distress as assessed by lung ultrasound versus thoracic radiographs. *J Vet Emerg Crit Care* 2018;28:415 – 428.

21. Martindale JL, Wakai A, Collins SP, etal. Diagnosing acute heart failure in the emergency department: a systematic review and meta-analysis. *Acad Emerg Med*. 2016:23;223 - 242.

22. Hori Y, Yamashita Y, Sakakibara K, et al. Usefulness of pericardial lung ultrasonography for the diagnosis of cardiogenic pulmonary edema in dogs. *Am J Vet Res* 2020;81: 227 - 232.

23. Feissel M, Maizel J, Robles G, et al. Clinical relevance of echocardiography in acute severe dyspnea. *J Am Soc Echocardiogr* 2009:22;1159 – 1164.

24. Fine DM, DeClue AE, Reinero CR. Evaluation of circulating amino terminal-pro-B-type natriuretic peptide concentration in dogs with respiratory distress attributable to congestive heart failure or primary pulmonary disease. *J Am Vet Med Assoc* 2008;232:1674 – 1679.

25. Oyama MA, Fox PR, Rush JE, et al. Clinical utility of serum N-terminal pro-B-type natriuretic peptide concentration for identifying cardiac disease in dogs and assessing disease severity. *J Am Vet Med Assoc* 2008;232:1496 – 1503.

26. Johnson EG, Wisner ER. Advances in respiratory imaging. *Vet Clin North Am Small Anim Pract*. 2007:37(5);879 - 900.

27. Masseau I, Reinero CR.Thoracic computed tomographic interpretation for clinicians to aid in the diagnosis of dogs and cats with respiratory disease. *Vet J*. 2019:253;1053 -88.

28. Labovitz AJ, Noble VE, Beirig M, et al. Focused cardiac ultrasound in the emergent setting: a consensus statement of the American Society of Echocardiography and American College of Emergency Physicians. *J Am Soc Echocardiogr* 2010;23:1225 – 30.

29. Tse YC, Rush JE, Cunningham SM, et al. Evaluation of a training course in focused echocardiography for noncardiology house officers. *J Vet Emerg Crit Care*. 2013; 23(3):268 - 73.

TABLES AND FIGURES

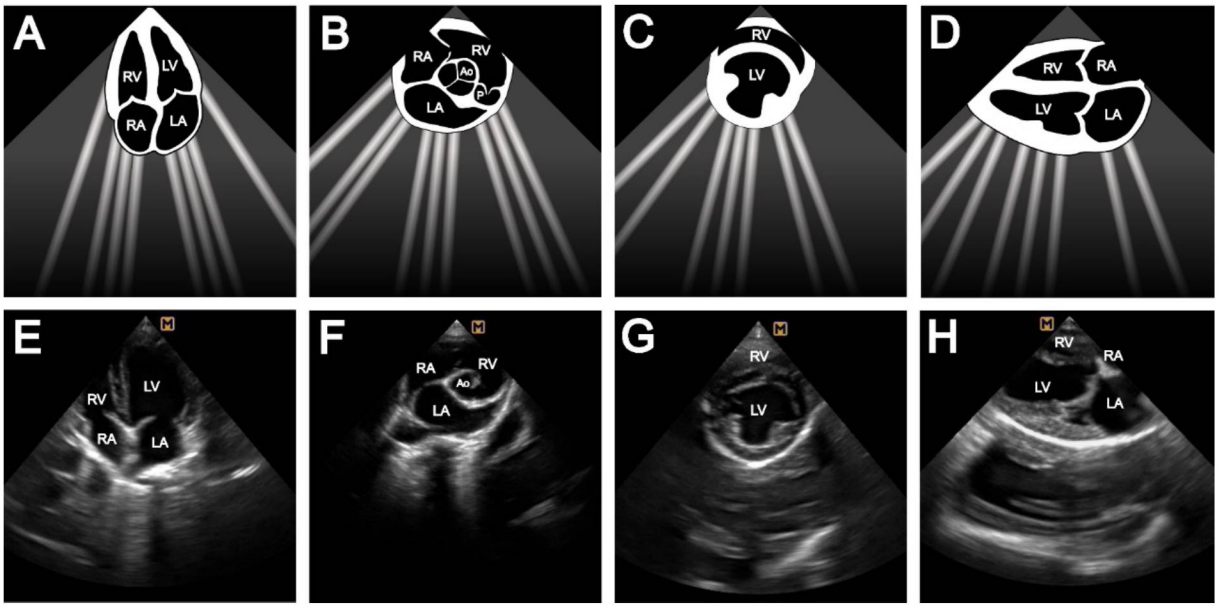

Figure 1 - A schematic ilustration of the 4 adapted echocardiographic views used in this study, with B lines arising from the pericardial-lung interface, above each corresponding echocardiographic image. A and E: Left parasternal apical 4 chambers view (LPA4C); B and F: Right parasternal short axis at aortic level (RPSAo); C and G: Right parasternal short axis at papillary muscle level (RPSPM); and D and H: Right parasternal long axis 4 chambers view (RPL4C). Ao: aorta; LA: left atrium; LV: left ventricle; RA: right atrium; RV: right ventricle

Table 1 – Demographic data and echocardiographic variables in 15 chronic valvular heart disease (CVHD) stage B1 dogs (Control), 15 CVHD stage B2 dogs without increased left ventricular filling pressures (RM), 15 CVHD stage B2 dogs with increased left ventricular filling pressures (RM&CONG), 15 CVHD dogs in pulmonary edema (CPE) and 15 CVHD dogs with pulmonary disease (PD).

	Control		RM		RM&CONG		CPE		PD		p-value between groups*
	M	SD	M	SD	M	SD	M	SD	M	SD	
Age	5.6[a]	3.7	12,2[b]	3.3	12.3[b]	2.4	12.3[b]	2.4	13.1[b]	2.0	<0.001
Weight	7.8[a]	5.4	6.8[a]	3.4	6.8[a]	4.0	5.7[a]	2.6	6.6[a]	3.2	0.908
LA/Ao	1.1[a]	0.1	1.7[bc]	0.1	2.0[bd]	0.3	2.2[d]	0.4	1.3[ac]	0.2	<0.001
LVIDDn	1.4[a]	0.2	1.8[b]	0.1	2.1[b]	0.2	2.0[b]	0.3	1.3[a]	0.4	<0.001
Emax	68.3[a]	13.3	88.3[a]	20.0	156.0[b]	20.4	141.4[b]	26.8	64.0[a]	22.8	<0.001
E/IVRT	1.4[a]	0.4	1.8[a]	0.5	6.6[b]	3.2	6.4[b]	3.0	1.2[a]	0.6	<0.001

M:mean; SD: standard deviation; LA/Ao: left atrium to aortic ratio; LVIDDn: normalized left ventricular internal diameter in diastole; Emax: peak velocity of E wave of transmitral flow; E/IVRT peak velocity of E wave isovolumic relaxation time ratio.
*ANOVA ; different letters means significant differences in multiple comparations.

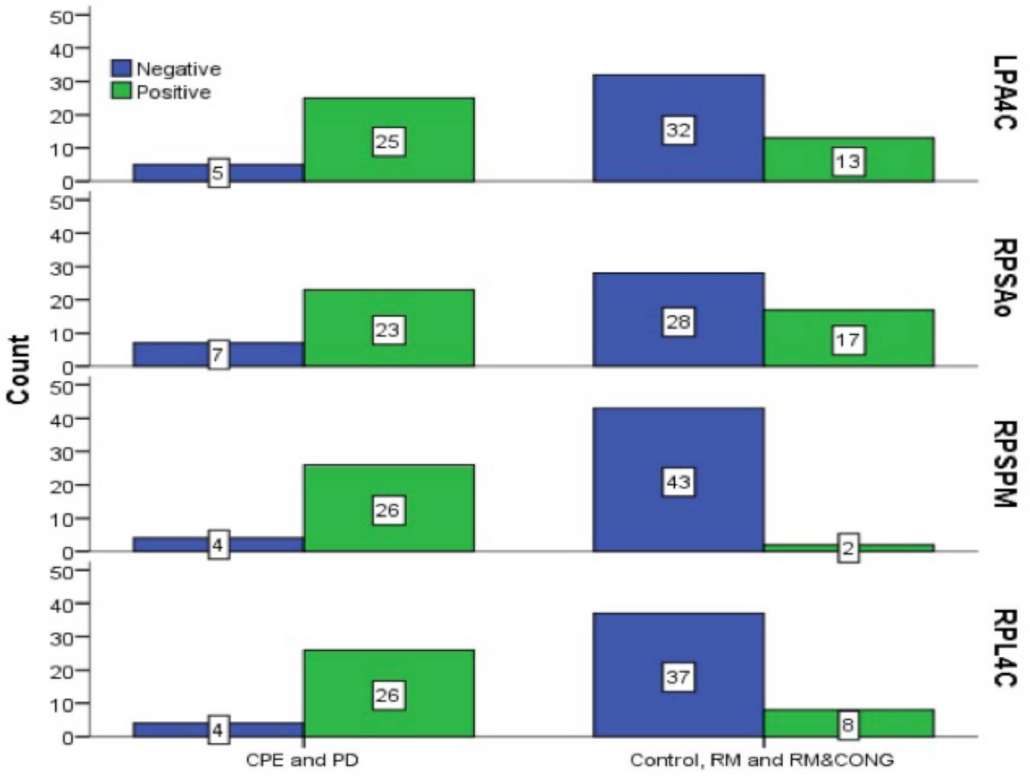

Figure 2 – Bar chart depicting the number of POSITIVE and NEGATIVE classifications in each one of the 4 views tested, when putting together groups with the same expected results (Control, RM and RM&CONG Vs. CPE and PD) LPA4C = Left parasternal apical 4 chambers view; RPSAo =Right parasternal short axis at aortic level RPSPM = Right parasternal short axis at papillary muscle level; RPL4C = Right parasternal long axis 4 chambers view.

Table 2 – Values of sensitivity, specificity, positive and negative predictive values and correct and incorrect classifications in dogs with cardiogenic pulmonary edema (CPE) or pulmonary disease (PD).

	Groups CPE and PD				
	Sn	**Sp**	**PPV**	**NPV**	**Accuracy**
LPA4C	83.3%	71.1%	65.8%	86.5%	76.0%
RPSAo	76.7%	62.2%	57.5%	80.0%	68.0%
RPSPM	86.7%	95.6%	92.9%	91.5%	92.0%

RPL4C	86.7%	82.2%	76.5%	90.2%	84.0%

CPE: cardiogenic pulmonar edema; PD: pulmonar disease; Sn: Sensitivity; Sp: Specificity; PPV: Positive predictive value; NPV: Negative predictive value; LPA4C: Left parasternal apical 4 chambers view; RPSAo: Right parasternal short axis at aortic level RPSPM: Right parasternal short axis at papillary muscle level; RPL4C: Right parasternal long axis 4 chambers view

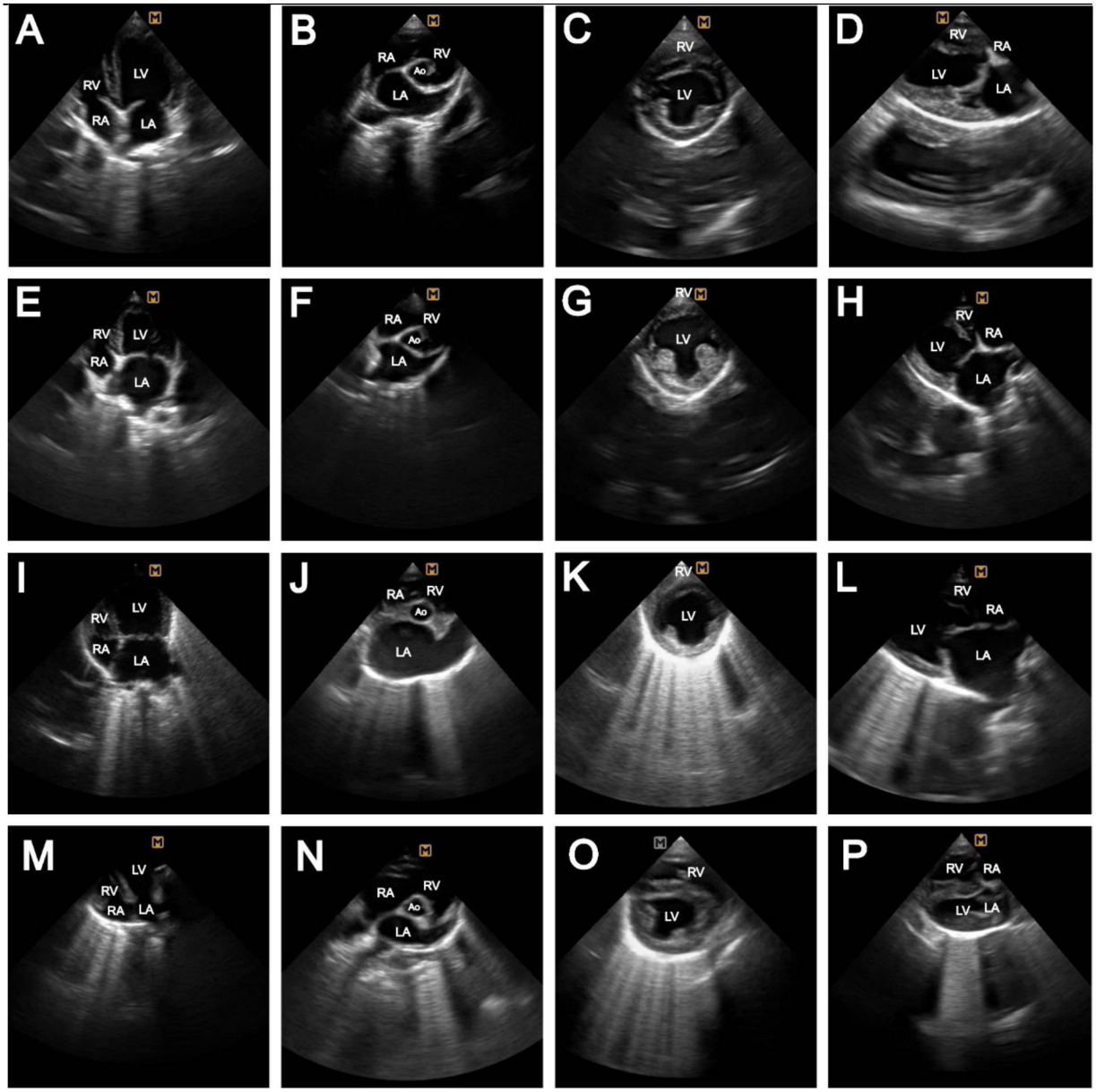

Figure 3 – Composition of 16 images showing the presentation of B lines in different clinical situations, in all 4 adapted echocardiographic views, from 4 dogs belonging to 4 different groups. A to D: Control; E to H: Remodeled (RM); I to L: Cardiogenic pulmonary edema (CPE); M to P: Pulmonary disease (PD); Ao: aorta; LA: left atrium; LV: left ventricle; RA: right atrium, RV: right ventricle.

Table 3 – Values of sensitivity, specificity, positive and negative predictive values and accuracy of multivariate analyses when combining a positive classification (> 3 B lines) and selected echocardiographic variables to distinguish dogs with cardiogenic pulmonary edema (CPE) from dogs with pulmonary disease (PD).

	CPE vs. PD when RPSPM and RPL4C are POSITIVE					
	Sn	**Sp**	**PPV**	**NPV**	**Accuracy**	**P-value**
RPSPM positive + LA/Ao > 1.6	100.0%	83.3%	87.5%	100.0%	92.3%	<0.001
RPL4C positive + LA/Ao > 1.6	100.0%	83.3%	87.5%	100.0%	92.3%	<0.001
RPSPM positive + LA/Ao > 2	64.3%	100.0%	100.0%	70.6%	80.8%	0.002
RPL4C positive + LA/Ao > 2	64.3%	100.0%	100.0%	70.6%	80.8%	0.002
RPSPM positive + Emax > 1.0 m/s	100.0%	91.7%	93.3%	100.0%	96.1%	<0.001
RPL4C positive + Emax > 1.0 m/s	100.0%	91.7%	93.3%	100.0%	96.1%	<0.001
RPSPM positive + Emax > 1.3 m/s	64.3%	100.0%	100.0%	70.6%	80.8%	0.002
RPL4C positive + Emax > 1.3 m/s	64.3%	100.0%	100.0%	70.6%	80.8%	0.002
RPSPM positive + E/IVRT > 2,5	100.0%	100.0%	100.0%	100.0%	100.0%	<0.001
RPL4C positive + E/IVRT > 2.5	100.0%	100.0%	100.0%	100.0%	100.0%	<0.001

CPE: cardiogenic pulmonary edema; PD: pulmonary disease; Sn: Sensitivity; Sp: Specificity; PPV: Positive predictive value; NPV: Negative predictive value; RPSPM: Right parasternal short axis at papillary muscle level; RPL4C: Right parasternal long axis 4 chambers view; LA/Ao: left atrium to aortic ratio; Emax: peak velocity of E wave of transmitral flow; E/IVRT peak velocity of E wave isovolumic relaxation time ratio.

CHAPTER 2 - Frontal QRST Angle as a Marker of Arrhythmogenesis and Disease Progression in Dogs with Myxomatous Mitral Valve Disease[1]

[1] *Written in accordance with the guidelines of Journal of Veterinary Cardiology, available in https://www.elsevier.com/journals/journal-of-veterinary-cardiology/1760-2734/guide-for-authors*

ABSTRACT

Introduction/Objectives: To investigate if an increased frontal QRST angle (fQRSTa) identifies ventricular arrhythmias in dogs with myxomatous mitral valve disease and to assess its role as a marker of disease progression.

Animals, Materials and Methods: 106 dogs with myxomatous mitral valve disease and 20 control dogs underwent clinical and echocardiographic examination, along with 3-minute electrocardiographic recordings. The fQRSTa was calculated for each one of the 126 dogs. Increases between disease stages were investigated, along with possible correlations of the fQRSTa and electrocardiographic variables related to increased arrhythmogenesis. Interclass and intraclass correlation tests were applied to investigate repeatability. Finally, sensitivity and specificity of fQRSTa in identifying arrhythmias and cardiac remodeling was calculated.

Results: An increase related to disease progression was documented for fQRSTa, with significant difference between groups C and B2 from Control, and group C from B1. A fQRSTa > 126.5 was able to discriminate B1 and Control from B2 and C dogs with a sensitivity of over 79% and specificity of 60.66%. A fQRSTa > 122.00 also discriminated the presence of arrhythmias from absolute sinus rhythms with a sensitivity of 88.24% and specificity of 70.00%. Finally, the index showed excellent repeatability, and positive correlations with previously reported ECG markers of arrhythmogenesis in dogs with myxomatous mitral valve disease.

Conclusion: The fQRSTa is positively related to arrhythmogenesis and cardiac remodeling in dogs with MMVD. Stages B2 and C MMVD dogs show increased fQRSTa, which allows to infer that repolarization is affected as disease progresses.

KEYWORDS: arrhythmias, electrocardiography, repolarization

Abbreviations

ACVIM	American College of Veterinary Internal Medicine
AUC	area under the curve
fQRSTa	frontal QRST angle
ECG	electrocardiogram
LA/Ao	ratio of the left atrial to aortic root diameters
MMVD	myxomatous mitral valve disease
nLVDd	normalized left ventricular internal diameter at end-diastole
ROC	receiver operating characteristic
Tpte	T-wave peak-end interval
Tpte/QT	ratio of T-wave peak-end interval and QT interval
VA	ventricular arrhythmias
VPCs	ventricular premature complexes

INTRODUCTION

Structural heart disease is the number one cause of sudden unexpected death in dogs [1]. Myxomatous mitral valve disease (MMVD) is well established as the most frequent acquired cardiac disease in this species, accounting for around 75% of heart disease in documented populations [2]. Although congestive heart failure is the main concern in this disease, dogs with MMVD have an increased risk of sudden cardiac death from ventricular arrhythmias (VA), and research involving electrocardiography (ECG) and Holter recordings have documented that VA become significantly more frequent as the disease progresses [3].

It is assumed that unstable repolarization dynamics play a major role in the genesis of VA in dogs with structural heart disease [4;5], especially due to the increased beat-to-beat variability of repolarization secondary to cardiac remodeling [6]. The elucidation of the electrophysiological events involved in rhythm disorders may lead to the identification of ECG markers that provide early identification of life-threatening arrhythmias, resulting in improved strategies for prevention and/or optimized clinical approach [7]. Recently, our group has investigated novel ECG variables that reflect impaired repolarization, especially due to their prognostic value, along with their inexpensive, noninvasive and quick-to-perform nature. Markers including prolongation and instability of the QT interval, as well as T-wave peak-end interval (Tpte) and the ratio of T-wave peak-end intervals and QT intervals (Tpte/QT) have all showed positive correlations with arrhythmogenesis, as well as prognostic value in dogs with

MMVD [8;9] In humans, the frontal QRST angle (fQRSTa) is a known repolarization parameter derived from vectorcardiography that reflects transmural dispersion, and its use as a marker of VA plays a role in risk stratification in a variety of clinical settings [10; 11; 12] Nonetheless, the use of fQRSTa in veterinary medicine is yet to be documented.

In this study, the authors hypothesized that MMVD dogs would exhibit an increased fQRSTa along with disease progression, making them more prone to developing VA. Therefore, the purpose of this study was to investigate possible correlations of increased fQRSTa and cardiac remodeling, and to assess the role of this variable as a marker of arrhythmogenesis in this disease.

ANIMALS, MATERIAL AND METHODS

Dogs recruited for this prospective cross-sectional observational study were selected among patients admitted for regular cardiac evaluation at a wide range of private veterinary clinics. All procedures received verbal client consent and were previously approved by the institutional Animal Use Committee, which complied with the National Institutes of Health Guide for the Care and Use of Laboratory Animals.

Among the inclusion criteria, the diagnosis of MMVD at any stage was required, which was based on clinical history and the echocardiographic criteria of impaired valvar anatomy and function [13]. Dogs with echocardiographic evidence of any congenital or acquired cardiac disease other than MMVD were excluded from the study, along with patients with bundle branch block on ECG, and patients undergoing antiarrhythmic therapy. Dogs with clinical and/or laboratorial evidence of debilitating systemic diseases at the time of diagnosis were also not included. Finally, healthy dogs that lacked valvar thickening where also gathered to be used as controls. Echocardiographic parameters such as left atrium-to-aorta ratio (LA/Ao) and normalized left ventricular internal diameter at end-diastole (nLVDd) were recorded for each dog [14]. The LA/Ao was measured in a two-dimensional short axis view obtained from the right paresternal window and calculated using a previously described method [15]. Cardiac

remodeling was defined as LA/Ao > 1.6 and nLVDd > 1.7 [2] All echocardiograms were carried out by two experienced veterinary cardiologists using an ultrasonography system (MySono U6 – Samsung, Suwon, South Korea) equipped with 3.0-8.0 MHz and 2.0-4.0 MHz phased array transducers (P2-4 and P3-8 reference – Samsung, Suwon, South Korea). Also, ECG tracings were acquired for each patient using a computer-based 6 lead surface ECG (InCardio® – Inpulse Animal Health Ltda., São Paulo, SP, Brazil), with the dogs placed in right lateral recumbency and maintained in position by gentle physical restraint. Alcohol was applied to the electrodes to improve electrical conduction. ECG was performed continuously and uninterrupted for three minutes.

The fQRSTa was calculated for each dog, which is represented by the absolute value of the difference between QRS axis and T-wave axis [10]. Whenever the difference exceeded 180 degrees, the fQRSTa was calculated as 360° minus the absolute value of the difference between the frontal plane QRS axis and T axis [11]. The calculation of the axis using the InCardio® software was semi-automatized, with the possibility of manually adjusting the reference line and wave intervals as needed. The QRS duration was defined as the interval from the start of the QRS complex until the J point. The T wave was defined as the interval from the first deflection, back to the point where it reaches the reference-line, with no future deflection (in case of biphasic morphologies). Positive, negative, and biphasic T waves were accepted. The step-by-step calculation of the fQRSTa in two canine ECGs with different T wave morphologies are shown in Figures 1 and 2. Also, whenever non-sinus rhythms or ectopic ventricular depolarizations occurred, they were recorded for future analyses, along with the prevailing baseline sinus rhythms. Other known electrocardiographic variables that reflect impaired repolarization such as T-wave peak-end interval (Tpte) and the ratio of T-wave peak-end intervals and QT intervals (Tpte/QT) in leads II and aVR were calculated, using a previously reported technique [9]. A single investigator, who was also blinded to the patient's heart condition, was responsible for all ECG measurements. Finally, 19 out of 126 (15%) animals were randomly selected for remeasuring and a second investigator was then recruited to determine the fQRSTa in these selected patients, to check for intra an interobserver

repeatability, respectively.

For statistical purposes, the dogs were divided in accordance with the stage of MMVD (B1, B2 and C) proposed by the consensus statement of the American College of Veterinary Internal Medicine [2], which depended on clinical signs attributable to congestive heart failure, as well as the echocardiographic evidence of cardiac remodeling. Healthy dogs that lacked valvular thickening were used as Controls. All data underwent the Shapiro-Wilk normality test. An analysis of variance followed by Tukey´s multiple comparison test was used to investigate differences between disease stages in the studied population. Pearson's test was used to assess whether correlations existed between fQRSTa and/or age and body weight, as well as between LA/Ao, nLVDd, Tpte (lead II), Tpte/QT (lead II), Tpte (aVR) and Tpte/QT (aVR). Interclass and intraclass correlation coefficient tests were applied to determine Cronbach's alpha and check index repeatability. Finally, receiver operating characteristic (ROC) curves were constructed to investigate sensitivity and specificity of fQRSTa to differentiate dogs with and without previously recognized arrhythmias, and to distinguish patients with dilated hearts from those without remodeling. All analyses were performed using the software GraphPad Prism (version 9.0 - San Diego, CA, USA) and Statistica (Version 10 - TIBCO Software, California, USA) using default settings The level of significance was defined as $P<0.05$.

RESULTS

One-hundred-and-twenty-six client-owned dogs were recruited by the end of the study. Although mixed breed dogs were the majority of the studied population (24.0%), several breeds were represented, including Miniature Poodle (18.4%), Lhasa Apso (12.0%), Shih-tzu (12.8%), Malteese (9.6%), Dachshund (4.8%), Yorkshire terrier (4.8%), Miniature Schnauzer (2.4%), French Bulldog (2.4%), German Spitz (1.6%), Pincher (1.6%), Cocker Spaniel (1.6%), Pug (0.8%), Whippet (0.8%), Bichon Frisé (0.8%) and Cotton de Tulear (0.8%). The age and body weight of the animals ranged from 1-17 years and 1.8-16 kg, respectively. Forty-two out of 126, 34/126 and 30/126 dogs were classified as stages B1 (32.8%), B2 (28,0%) and C

(23.2%), respectively, along with 20/126 Controls (16.0%). No difference existed between stages regarding sex (P=0.0527), weight (P=0.4744), but a significant and expected age difference was documented between the controls and all the other groups (P=0.0001). Demographic data is summarized in Table 1.

When it comes to rhythm analyses, sinus arrhythmia was the predominant background rhythm. Ten of 126 dogs (7.9%) had ventricular premature complexes (VPCs), all of which presented with a right bundle branch block morphology. Six of them (60%) were classified as ACVIM stage C patients, three (30%) were B2, and one (10%) was B1. All VPCs identified were isolated, except for one stage C dog that presented a paroxysmal ventricular tachycardia. The occurrence of supraventricular arrhythmias was also higher in stage C patients (four dogs [13.3%] with atrial fibrillations and 3 dogs [10%] with atrial premature complexes). One stage C patient (0.33%) had both atrial fibrillation and VPCs. Two stage B2 patients (0.58%) had atrial premature complexes and one (0.29%) had atrial fibrillation. Therefore, a total of 19/126 patients (15%) were identified with arrhythmias of non-sinus origin during ECG recording, none of which was from the Control group.

The fQRSTa showed a significant difference between Controls and B2 and C, and also between B1 and C. No significant difference was found between groups Control and B1, as well as between B1 and B2 (p=0.0001). The mean values of the index for each group increased from 74.90 (Control) to 149.07 (C), as shown in the box-plots in Figure 3.

Regarding correlations, fQRSTa was positively correlated with LA/Ao (ρ = 0.3900), Tpte(lead II) (ρ = 0.3411), Tpte/QT (lead II) (ρ = 0.3134), Tpte(avR) (ρ = 0.3801) and Tpte/QT (aVR) (ρ = 0,3811). Significant correlations are represented as Scatter Plots in Figure 4.

For repeatability assessment, the interclass and intraclass correlation coefficient test generated Cronbach`s Alpha of 0.987 and 0.903 for intraobserver and interobserver variability, respectively, with P = 0.0001

Finally, regarding ROC curves, an area under the curve (AUC) of 0.8000 was obtained when using fQRSTa to differentiate dogs with rhythm disorders from dogs in the Control group with absolute sinus rhythms at the time of diagnosis. Also, to distinguish dogs with remodeled

hearts from those without remodeling, an AUC of 0.6707 was documented. The corresponding curves are shown in Figure 5. The best cut-off values to identify remodeling and rhythm disorders, with the respective sensitivity, specificity, and odds ratio values are shown in Tables 2 and 3.

DISCUSSION

In this investigation, we sought to assess fQRSTa in dogs with MMVD to identify repolarization instabilities in the ventricular myocardium. Our results demonstrated that fQRSTa, a marker of impaired repolarization in medicine, is not only a marker of arrhythmogenesis in MMVD dogs, but also identifies disease progression.

The fQRSTa is derived from vectorcardiography, a method that is based on the identification of heart vectors through cardiac cycle as loops. The QRS loop reflects depolarization, whereas the T loop reflects repolarization. By vectorcardiography, it is possible to measure a spatial angle between depolarization and repolarization, or, in other words, an angle between the QRS and T vector. Projection of three-dimensional spatial QRS and T vectors onto the frontal plane produces the fQRSTa [16]. An abnormally wide fQRSTa reflects impaired repolarization dynamics, and a series of studies have shown that this finding stratifies arrhythmogenic risk in a variety of medical settings [10; 11; 12]. Hence, the clinical use of this resource may impact upon decision making when it comes to selecting patients that would benefit from a cardioverter inplantaion in the general population [17].

In MMVD dogs, although precise mechanisms are yet to be underlined, the etiology of VA seems multifactorial, and includes anatomical substrate (myocardial stimulation through prolapsed leaflets and ventricular dilation) and a disrupted autonomic nervous system, similar to mitral valve prolapse in humans [18]. At a cellular level, in chronic structural heart diseases, there is an increase in beat-to-beat variability in an otherwise uniform action potential duration, resulting from increased membrane instability [19]. Recent studies have shown that repolarization disorders are exposed in the ECG in the form of progressive prolongation and

instability of the QT interval, as well as increases in Tpte and Tpte/QT [8,9]. These findings most likely explain the impaired repolarization dynamics involved in the generation of VA in MMVD dogs, which become significantly more prevalent with disease progression [3].

In our study, when used to identify rhythm disorders, the fQRSTa produced a ROC curve with an AUC of 0.8000 when discriminating dogs with arrhythmias from those of the Control group with absolute sinus rhythms. Dogs with fQRSTa >122.0 (sensitivity: 88.24% / specificity: 70.00%) were shown to be more prone to developing rhythm disorders. In addition, our study identified significant correlations of fQRSTa with previously documented ECG markers of VA in MMVD, such as Tpte [9]. This finding strengthens the role of this variable as a marker of arrhythmogenesis in canine valvular degeneration.

Also, fQRSTa discriminated MMVD dogs with remodeled and non-remodeled hearts. A fQRSTa > 126.5 was able to discriminate B1 and Control from B2 and C dogs with a sensitivity of 79.7% and specificity of 60.7%, with dogs being 4.5 times more likely to exhibit cardiac dilatation. Although echocardiography remains the gold standard for evaluation of cardiac anatomy and function, markers of remodeling obtainable from conventional ECG tracings may aid in clinical screening when echocardiography in unavailable. Also, the identification of significant correlations of fQRSTa and LA/Ao supports the finding that the fQRSTa increases with disease progression. In severe cases of mitral valve regurgitation, volume overload leads to left atrial remodeling and increases left atrial filling pressure, which are all associated with the onset of clinical signs of heart failure [20]. The significant correlation with LA/Ao is supportive of repolarization disorders increasing as clinical signs become overt [19].

An important limitation of this research involves the use of standard ECG recordings, instead of a 24-hour Holter monitoring. As we know, the paroxysmal nature of most arrhythmias may lead to false negative diagnosis when relying upon 3-minute tracings. The use of a 24-hour Holter monitoring would certainly improve identification of rhythm disorders, leading to an increase in sensitivity and specificity values. Another limitation is related to the measurings relying on the use of a specifc software, attributed to its corresponding digital ECG machine.

From this point, there is no way to predict how the index will behave in equipments from different vendors. Lastly, the true prognostic potential of this index in predicting the development of arrhythmias and sudden cardiac death requires future longitudinal studies.

CONCLUSIONS

Although sudden cardiac death is not considered a common outcome in MMVD patients, it's surely the most devastating complication, and it is agreed that VA play a major role [1,3]. This study has shown that fQRSTa increases with progression of MMVD in dogs, and may detect increased predisposition to arrhythmia development in this patients. Values for fQRSTa of 122 and 126 performed as the most precise cuttoffs to identify the presence of rhythm disorders and remodeling, respectively. The prognostic applicability of fQRSta in dogs with MMVD is yet to be investigated.

REFERRENCES

1. Olsen TF, Allen AL. Causes of sudden and unexpected death in dogs: a 10-year retrospective study. Can Vet J 2000;41:873e5.
2. Keene BW, Atkins CE, Bonagura JD, Fox PR, Haaggstrom J, Fuentes VL, Oyama MA, Rush JE, Stepien R, Uechi M. ACVIM consensus guidelines for the diagnosis and treatment of myxomatous mitral valve disease in dogs. J Vet Intern Med 2019;33:1127e40.
3. Crosara S, Borgarelli M, Haggstrom J. Holter monitoring in 36 dogs with myxomatous mitral valve disease. The Journal of the Australian Veterinary Association, 2010 v. 88, n.10, p.386-391
4. Berger R, Kasper E, Baughman K, Marban E, Calkins H, & Tomaselli G. Beat-to- beat QT interval variability. Novel evidence for repolarization lability in ischemic and nonischemic dilated cardiomyopathy. Circulation, 1997 96, 1557– 1565.

5. Barr CS, Naas A, Freeman M, Lang CC, Struthers AD. QT dispersion and sudden unexpected death in chronic heart failure. Lancet 1994;343:327e9.
6. Thomsen B, Truin M, Opstal JM, Beekman JD, Volders PG, Stengl M, Vos MA. Sudden cardiac death in dogs with remodeled hearts is associated with larger beat-to-beat variability of repolarization. Basic Res Cardiol 2005;100: 279e87.
7. Chen X, Tereshchenko LG, Berger RD, Trayanova NA. Arrhythmia risk stratification based on QT interval instability: an intracardiac electrocardiogram study. Heart Rhythm 2013;10:875e80.
8. Brüler BC, Jojima FS, Dittrich G, Giannico AT, Sousa MG. QT instability, an indicator of augmented arrhythmogenesis, increases with the progression of myxomatous mitral valve disease in dogs. J Vet Cardiol 2018;20:254e66.
9. Vila BC, Camacho AA, Sousa MG. T-wave peak-end interval and ratio of T- wave peak-end and QT intervals: novel arrhythmogenic and survival markers for dogs with myxomatous mitral valve disease. Journal of Veterinary Cardiology 2021 35, 25e41
10. Chua KCM, Teodorescu C, Reinier K, et al. Wide QRST angle on the 12-Lead ECG as a predictor of sudden death beyond the LV ejection fraction. J Cardiovasc Electrophysiol. 2016;27:833-839.
11. Borleffs CJ, Scherptong RW, Man SC, et al. Predicting ventricular arrhythmias in patients with ischemic heart disease: clinical application of the ECG-derived QRS-T angle. Circ Arrhythm Electrophysiol 2009;2:548–554.
12. Palaniswamy C, Singh T, Aronow WS, et al. A planar QRS-T angle> 90 degrees is associated with multivessel coronary artery disease in patients undergoing coronary angiography. Med Sci Monit. 2009;15: MS31-MS34.
13. Chetboul, V., Tissier, R.. Echocardiographic assessment of canine degenerative mitral valve disease. Journal of Veterinary Cardiology 201214, 127-148
14. Cornell CC, Kittleson MD, Della Torre P, Haggstrom J, Lombard CW, Pedersen HD, Vollmar A, Wey A. Allometric scaling of M-mode cardiac measurements in normal adult dogs. J Vet Intern Med 2004;18:311e21.

15. Hansson K, Haggstrom J, Clarence K, Lord B Left atrial to aortic root indices using two-dimensional and m-mode echocardiography in cavalier king charles spaniels with and without left atrial enlargement. Vet Radiol Ultrasound. 2002 Nov-Dec;43(6):568-75.
16. Oehler A, Feldman T, Henrikson C, Tereshchenko L. QRS-T Angle: A Review. Ann Noninvasive Electrocardiol 2014;19(6):534–542.
17. Güner A, Kalçık M, Çelik M, et al., Impaired repolarization parameters may predict fatal ventricular arrhythmias in patients with hypertrophic cardiomyopathy (from the CILICIA Registry), Journal of Electrocardiology (2020), https://doi.org/10.1016/j.jelectrocard.2020.10.009
18. Zuppiroli A, Mori F, Favilli S, et al. Arrhythmias in mitral valve prolapse: relation to anterior mitral leaflet thickening, clinical variables, and colour Doppler echocardiographic parameters. Am Heart J 1994; 128: 919–27.
19. Haigney MC, Wei S, Kaab S, et al. Loss of cardiac magnesium in experimental heart failure prolongs and destabilizes repolarization in dogs. J Am Coll Cardiol. 1998 31:701–706.
20. Reynolds CA, Brown DC, Rush JE Prediction of first onset of congestive heart failure in dogs with degenerative mitral valve disease: the PREDICT cohort study. Journal of Veterinary Cardiology 2012; 14, 193-202

TABLES AND FIGURES

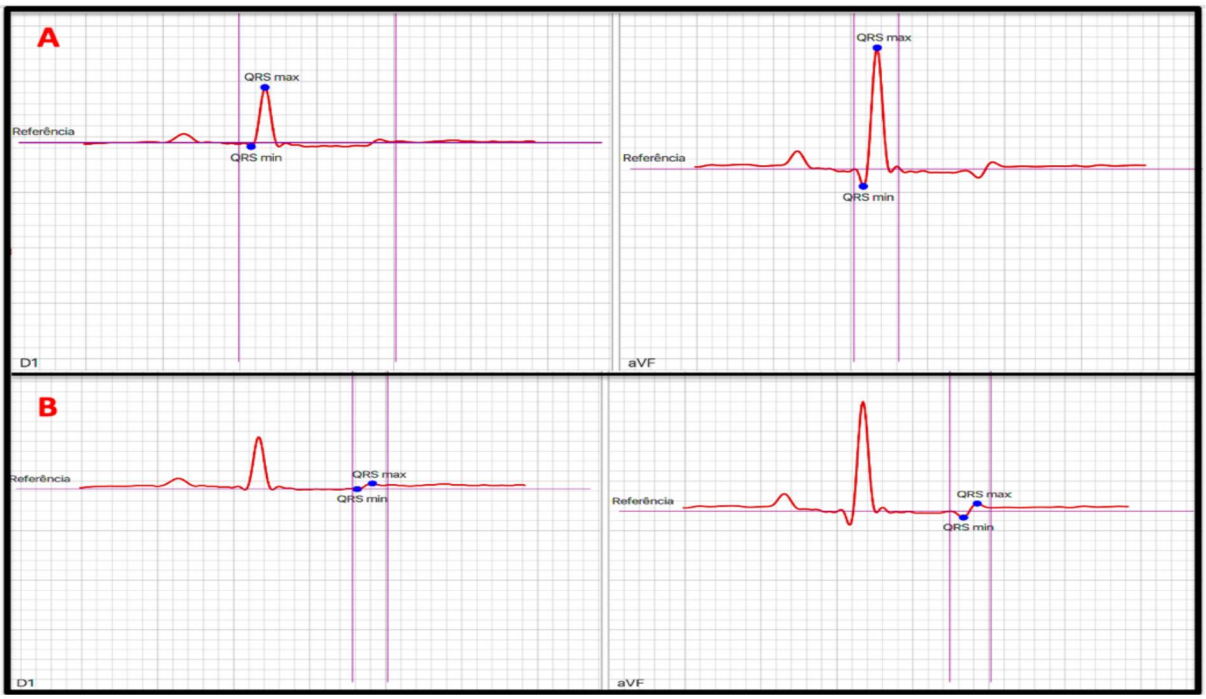

Figure 1 The semi-automated method for determining the QRS axis and the T wave axis through leads D1 and avF, using the software's tool originally built to determine the QRS axis. The T wave is defined as the interval from the first deflection, back to the point where it reaches the reference-line, with no future deflection (in case of biphasic morphologies). The peaks are defined as the time point where the T wave reaches the maximal and minimal amplitudes. The frontal QRST angle (fQRSTa) corresponds to the absolute value of the difference between the QRS axis and T-wave axis, corrected for it's smallest equivalent in 360 °. QRS axis in A = 67°. T wave axis in B = 15°. fQRSTa = 67 – 15 = 52 °

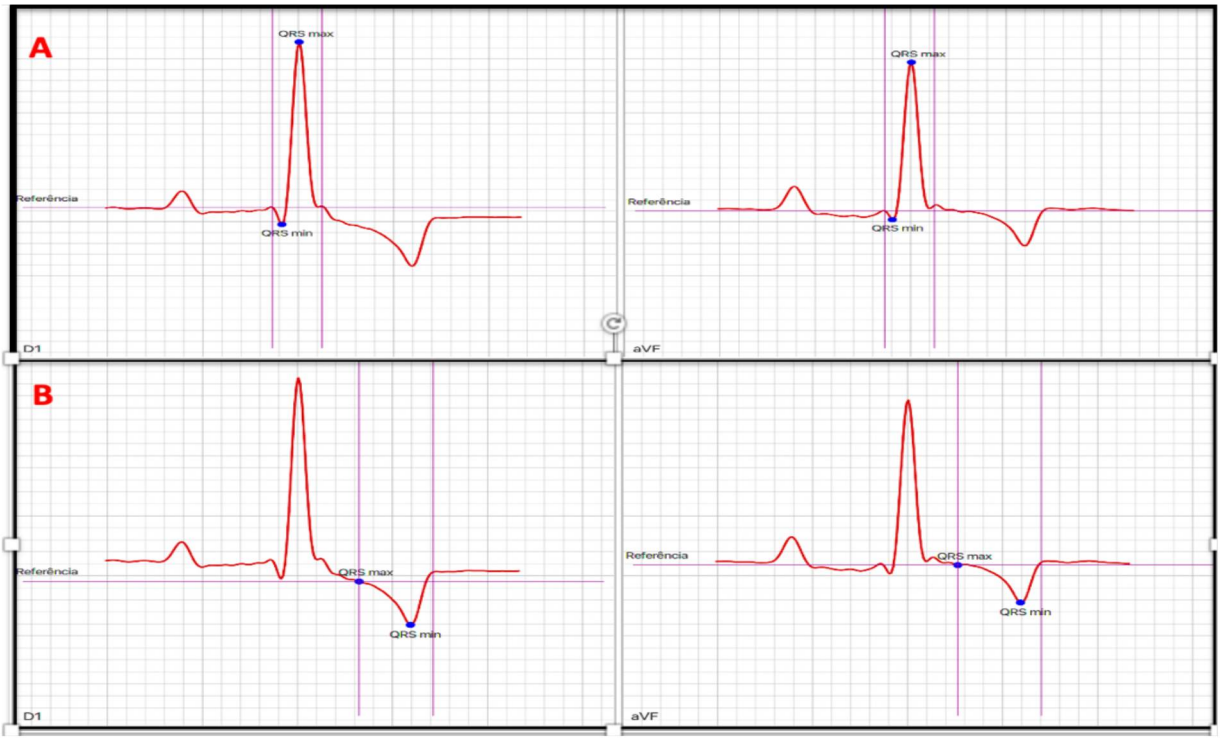

Figure 2 The semi-automated method for determining the QRS axis and theT wave axis through leads D1 and avF, using the software's tool originally built to determine the QRS axis. The T wave is defined as the interval from the first deflection, back to the point where it reaches the reference-line, with no future deflection (in case of biphasic morphologies). The peaks are defined as the time point where the T wave reaches the maximal and minimal amplitudes. The frontal QRST angle (fQRSTa) corresponds to the absolute value of the difference between QRS axis and T-wave axis, corrected for it's smallest equivalent in 360º. QRS axis in A = 47º. T wave axis in B = -135º. fQRSTa = 47 – (-135) = 182º. Correcting for the smallest equivalent in 360 º → fQRSTa = 178º

Table 1. Demographic features of healthy control dogs and dogs with MMVD.

Variables	Groups								Total		*p*
	B1		B2		C		Control				
	n	%	n	%	n	%	n	%	n	%	
Sex											
Male	24	19.2	20	16.0	9	7.2	7	5.6	60	48.0	0.0527
Female	17	13.6	15	12.0	20	16.0	13	10.4	65	52.0	
				Mean±SD							
Age (Years)	11.3±3.0[A]		12.5±2.3[A]		12.3±1.8[A]		5.5±3.0[B]		11.9±3.10		0.0001
Weight (Kg)	7.8±4.2		7.1±3.6		6.9±3.5		8.5±4.1		6.7±3.3		0.4744

Results of age and weight are presented as mean ± standard deviation. Values followed by the same letter do not differ from each other by chi-square test (p > 0.05).

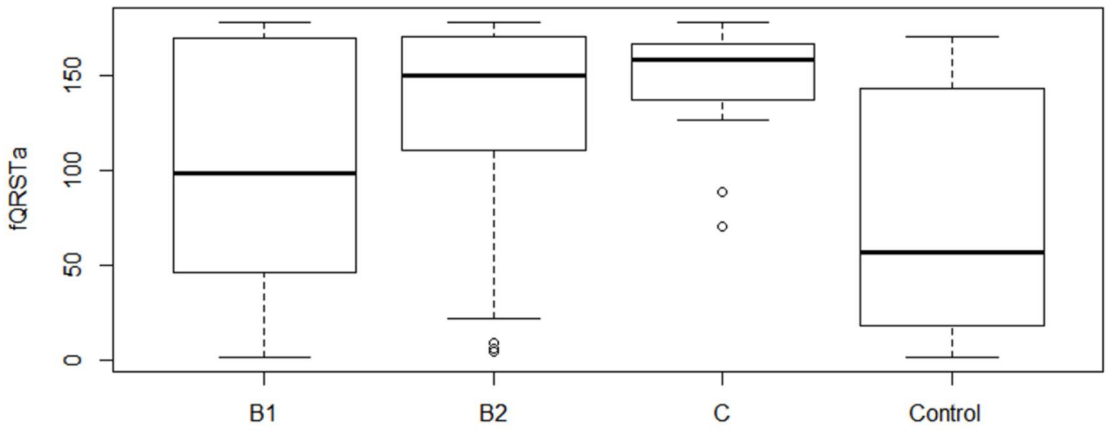

Figure 3. Box plots depicting the medians, interquartile ranges, and amplitude of the fQRSTa in dogs in different stages of myxomatous mitral valve disease and healthy control dogs. Outliers are shown. fQRSTa = frontal QRST angle.

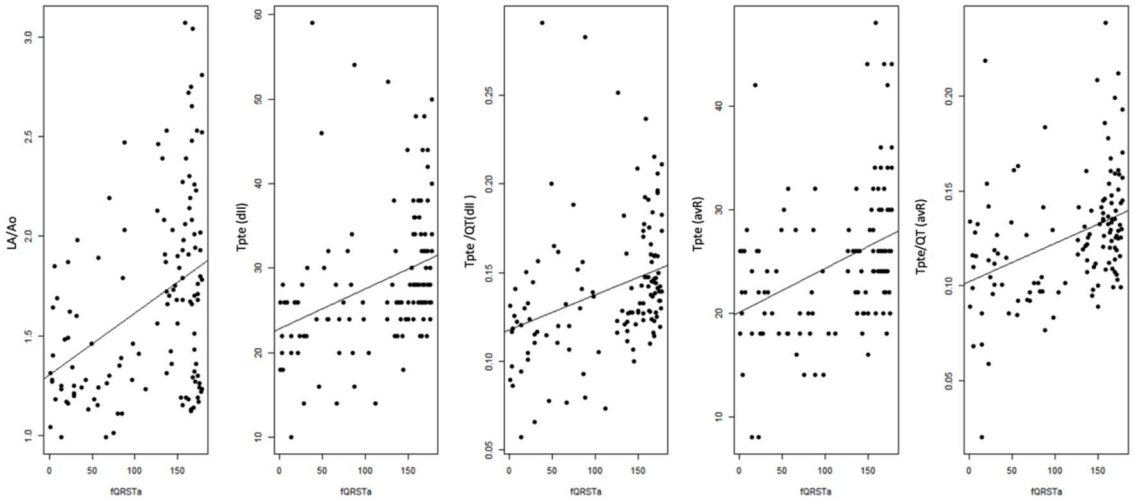

Figure 4 – Scatter-plots depicting significant positive correlations between fQRSTa and LA/Ao (ρ = 0.3900), Tpte(dII) (ρ = 0.3411), Tpte/QT(dII) (ρ = 0.3134), Tpte(avR) (ρ = 0.3801), Tpte/QT (avR) (ρ = 0,3811). LA/Ao ratio of the left atrial to aortic root diameters; Tpte: T-wave peak-end interval; Tpte/QT: Ratio of Tpte and QT intervals.

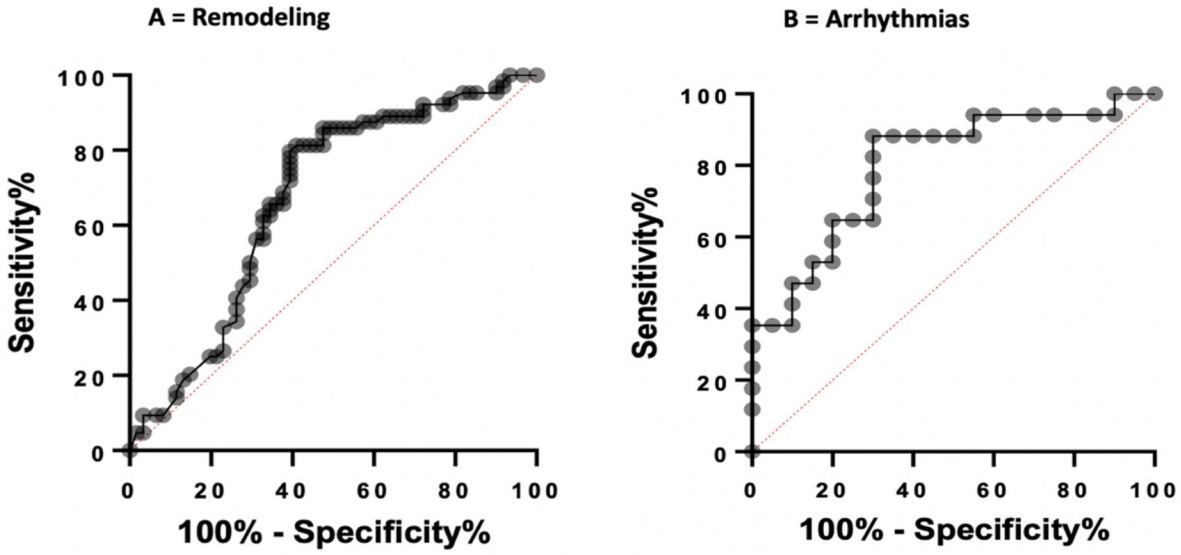

Figure 5 Receiver operating characteristic curves constructed to assess sensitivity and specificity of the fQRSTa in differentiating dogs with either remodeled (MMVD stages B2 and C) or non-remodeled (MMVD stage B1 and Control) hearts (AUC=0.6707) and sensitivity and specificity of the fQRSTa in differentiating dogs with and without arrhythmias (B) (AUC=0.8000). fQRSTa, frontal QRST angle; AUCs, areas under the curve.

Table 2 Cutoff values, sensitivity, specificity, positive predictive value (PPV), accuracy, and odds ratio obtained when using the fQRSTa to differentiate dogs with remodeled (MMVD stages B2 and C) and non-remodeled (MMVD stage B1 and Control) hearts.

Cutoff	Sensitivity%	Specificity%	PPV	Accuracy(%)	Odds ratio
> 21.00	95,31	18,03	92,86	20,80	1,72
> 23.00	93,75	21,31	94,12	23,20	2,19
> 126.5	79,69	60,66	96,00	48,00	4,57
> 169.5	20,31	85,25	90,29	77,60	2,07

> 170.5	18,75	86,89	90,48	79,20	2,38

fQRSTa = frontal QRST angle; PPV = positive predictive value

Table 3 Cutoff values, sensitivity, specificity, positive predictive value (PPV), accuracy, and odds ratio obtained when using the fQRSTa to differentiate dogs with arrhythmias from dogs from the Control group with only sinus rhythms.

Cutoff	Sensitivity%	Specificity%	PPV	Accuracy(%)	Odds ratio
> 86.00	88.24	60,00	14.29	27.03	0.09
> 104.5	88.24	65.00	13.30	24.32	0.07
> 122.0	88.24	70.00	12.50	21.62	0.06
> 142.5	64.71	75.00	28.51	29.72	0.18
> 146.5	64.71	80.00	27.27	27.02	0.14

fQRSTa = frontal QRST angle; PPV = positive predictive value

CHAPTER 3 An Overview of Myocardial Mechanics Through Two-Dimensional Speckle Tracking Echocardiography and Bulls-Eye Mapping in Dogs With Mitral Valve Disease.[1]

ABSTRACT

Introduction/Objectives: To evaluate myocardial mechanics and investigate the presence of global longitudinal, circumferential and/or regional systolic disfunction patterns and/or desynchrony through a visual bidimensional speckle tracking derived echocardiographic technique in dogs with myxomatous mitral valve disease of different severities.

Animals, Materials and Methods 40 dogs with myxomatous mitral valve disease that met study inclusion criteria underwent clinical examination, conventional and speckle tracking echocardiography, systemic blood pressure measurements and 3-minute ECG tracings. Bulls-eye diagrams of longitudinal and circumferential strain were obtained using apical 2, 3 and 4 chambers view, and transverse apical, mid and basal planes, respectively. Global and regional longitudinal and circumferential strain, as well as segmental peak strains of the different myocardial segments were also tabulated. Analysis of variance followed by Tukey's test was used to investigate differences between disease stages in the studied population, and Spearman's test was used to assess existing correlations of strain values and conventional echocardiographic variables related to cardiac remodeling and systolic function.

Results: Stages C and B2 patients had evidence of global circumferential systolic disfunction when compared to stage B1 patients, essentially due to regional differences in mid and basilar planes. This finding anticipated evidence of systolic dysfunction when compared to conventional echocardiographic parameters. No difference in global or regional longitudinal systolic function was detected between groups.

Conclusion: Global circumferential systolic function decreases with the development of

[1] *Written in accordance with the guidelines of Journal of Veterinary Cardiology, available in https://www.elsevier.com/journals/journal-of-veterinary-cardiology/1760-2734/guide-for-authors.*

cardiac remodeling in MMVD dogs, and impaired myocardial segments may be identified through bulls-eye mapping, prior to radial systolic disfunction analyzed in conventional echocardiographic studies.

KEYWORDS: strain, speckle tracking, mitral valve disease, myocardium

Abbreviations

ACVIM	American College of Veterinary Internal Medicine
ANT	anterior segment
ANT-LAT	Anterior lateral segment
ANT-SEPT	anterior septal segment
EF%	ejection fraction
Emax	peak velocity of mitral E wave
FS%	fractional shortening
INF	inferior segment
INF-SEPT	inferior septal segment
INF-LAT	inferior lateral segment
IVRT	isovolumic relaxation time
LA/Ao	ratio of the left atrial to aortic root diameters
MMVD	myxomatous mitral valve disease
nLVDd	normalized left ventricular internal diameter at end-diastole
SAX A	transversal apical plane
SAX B	transversal basal plane
SAX M	transversal mid plane

INTRODUCTION

Myxomatous mitral valve disease (MMVD) is the number one cause of mitral regurgitation in dogs and represents the most common acquired heart disease in this species, accounting for around 75% of heart disease in documented populations [1]. Although the pathophysiology essentially relies on the thickening and mis-coaptation of the valvular apparatus, progressive volume overload and cardiac stretching leads to structural changes in ventricular myocardial fibers, that may result in systolic disfunction with time [2,3,4]

Conventional echocardiographic studies, in addition to being the gold standard method for determining the diagnosis of MMVD, also provides important information for determining disease severity, such as the degree of left cardiac remodeling, indices of increased left ventricular filling pressures and the presence of systolic dysfunction [5,6]. This information is pivotal for determining medical therapy and the frequency of follow-up.

When it comes to the assessment of systolic function, however, standard echocardiographic variables that rely on conventional bi-dimensional (2D) and M-Mode techniques may be misleading, especially due to the changes in ventricular loading that accompany severe mitral regurgitation [7]. Shortening and ejection fractions, traditional measures of global systolic function, are highly influenced by preload and afterload, respectively. In addition, shortening and ejection fractions reflect essentially radial systolic function, that is known to be affected only in latter stages [8,9].

Systolic function determining techniques derived from speckle tracking are well known in medicine, although the literature is still scarce in veterinary medicine, particularly in dogs with MMVD [10,11]. Speckles are natural markers of myocardial tissue, derived from the reflection of the sound beam, which can be tracked during cardiac cycles, and reflect information about myocardial deformation [11,12]. Unlike Doppler derived techniques, the identification of speckles is independent of the ultrasound incidence angle, allowing the assessment of cardiac mechanics in 3 spatial planes (circumferential, longitudinal, and radial), as well as not being impacted by translational movement [13]. Circumferential and longitudinal strains are calculated as negative in systole and positive in diastole, with peak strain values

generally occurring near the end of ventricular ejection [12].

The bulls-eye mapping, a 2D speckle tracking derived technique, is a tool that reflects visual and quantitative information about global longitudinal and circumferential systolic function, through the mapping of the left ventricle and its arrangement in the form of a target [14]. The bulls-eye diagram divides the left ventricle in different myocardial segments, resulting in a 3-dimensional perspective of myocardial mechanics during systole, in the longitudinal and transversal plane. The resulting diagram gives consistent and visual information regarding global strain, as well as segmental myocardial mechanics, allowing the identification of desynchrony and patterns of systolic disfunction prior to clinical or conventional echocardiographic evidence [15]. Early and more precise information about left ventricular (LV) systolic function in MMVD might help us to better understand the natural history of this disease, offer more accurate prognoses and guide follow-up care.

Thus, the objective of this study was to evaluate longitudinal and circumferential systolic function and identify patterns of focal impairment by means of the bulls-eye mapping in dogs with MMVD of different severities, and to compare this information with conventional variables of LV remodeling and function.

ANIMALS, MATERIAL AND METHODS

Dogs recruited for this prospective cross-sectional observational study were selected among patients admitted for cardiac evaluation at a veterinary teaching facility. Dogs that lacked history of cardiovascular disease were referred because of a murmur auscultation during physical examination, while dogs with previous diagnosis of MMVD were evaluated for routine echocardiographic control or after manifesting signs of heart failure. All procedures were previously approved by the institutional Animal Use Committee and complied with the National Institutes of Health Guide for the Care and Use of Laboratory Animals.

To be included in the study, the diagnosis of MMVD was required, which was based on the echocardiographic criteria of impaired valvar anatomy and function [5]. Dogs with

echocardiographic evidence of any congenital or acquired cardiac disease other than MMVD were excluded from the study, along with patients with elevated systemic blood pressure (> 160 mmHg), patients with a history of severe systemic conditions, such as decompensated endocrinopathies or in treatment of malignant tumors. Once recruited, the dogs were subdivided based on the stage of MMVD (B1 B2 and C), according to up-to date ACVIM guidelines, which took into consideration the echocardiographic findings of cardiac remodeling and clinical status [1].

All echocardiograms were carried out by experienced veterinary cardiologists using an ultrasonography system (Philips Affiniti 50) equipped with 2-4 and 3-8 MHz phased array transducers. Dogs were positioned in right and left lateral recumbency and maintained in position by gentle physical restraint. No sedation was applied, and whenever a patient didn't generate good quality imagens, it was excluded from the study. All echocardiographic examinations and measurements were performed by the same operator, to avoid interobserver discrepancy. Echocardiographic measuring included normalized left ventricular diameter in diastole (nLVDd) [16] fractional shortening (FS%) and ejection fraction (EF%) (calculated by the Teichholz formula) obtained by M-mode from the right parasternal short-axis images. 2D short-axis images obtained from the right parasternal window were used to calculate the left atrium-to-aorta ratio (LA/Ao). Left apical 4-chambers (AP4) and 5-chambers view were used to record diastolic peak velocities of mitral E (Emax) and A waves, the E/A ratio and the isovolumic relaxation time. Also, the aortic valve closure time, which corresponds to the time from the beginning of the QRS complex to the end of the aortic valve spectra, was obtained by positioning the pulsed Doppler gate distal to the aortic valves.

After echocardiographic examination, 12-lead ECG tracings were acquired from each patient, with the dog positioned in right lateral recumbency and maintained in position by gentle physical restraint. Electrodes were attached to the skin and wet with alcohol to improve electrical conduction. ECG was performed continuously and uninterrupted for three minutes.

Once the patient was dismissed, post-acquisition measurements were applied to the recorded videos by the same researcher, and the bulls-eye diagram for longitudinal and

circumferential strain was obtained as follows:

Longitudinal bulls-eye mapping

From the left parasternal echocardiographic windows, two-dimensional apical-4-chambers (AP4), apical-2-chambers (AP2) and apical 3-chambers (AP3) videos of at least four cardiac cycles were registered. The machine software automatically identifies the left ventricular endocardium to be screened, with manual corrections enabled when tracking mistakes were identified by the observer. After the screening in 3 different planes, the software builds a target image of 16 different segments, grouped in 6 different myocardial regions, as follows: inferior septal (INF-SEPT), anterior septal (ANT-SPET), anterior (ANT), anterior lateral (ANT-LAT), inferior lateral (INF-LAT) and inferior (INF). For longitudinal strain, a central segment corresponding to the cardiac apex is also tracked. According to the longitudinal deformation of the fibers, the percent strain is automatically given for each segment. Finally, the strain values from all segments are averaged to obtain a global longitudinal strain (GLS) value, as well as the three regional strain values (AP2, AP3 and AP4 strain). The tracking of three apical views and the resulting bulls-eye target of longitudinal strain in depicted in Figure 1.

Transversal Bulls-eye mapping

From the right parasternal windows, two-dimensional transversal images of the ventricle in 3 different planes: apical, mid and basal plane videos were obtained for at least four cardiac cycles. Similar as discussed with the longitudinal bulls-eye mapping, the ventricular myocardium is automatically depicted in 16 myocardial segments, organized into INF-SEPT, ANT-SEPT, ANT, ANT-LAT, INF-LAT and INF cardiac regions. According to the circumferential deformation of the fibers, the percent strain is automatically given for each segment. Finally, strain values of each segment are averaged to obtain three regional circumferential strains (SAX A, SAX M and SAX B) and the global circumferential strain (GCS). The tracking of three different planes and the resulting bulls-eye target of circumferential strain in depicted on Figure 2.

All data underwent the Shapiro-Wilk normality test. An analysis of variance followed by Tukey´s multiple comparison test was used to investigate differences between groups. In addition, a Spearmans test was used to assess whether correlations existed between the circumferential and or longitudinal strain and conventional echocardiographic parameters. All analyses were performed using the softwares GraphPad Prism (Version 9.0 - San Diego, CA, USA) and Statistica Single User version 13.2 using default settings. For all analyses, the level of significance was defined as $P<0.05$.

RESULTS

In this investigation, we tested a contemporary echocardiographic technique to evaluate myocardial mechanics and systolic function in dogs with MMVD of different stages, which consists of a two-dimensional speckle-tracking strain analyses called the bulls-eye mapping. Fourty client-owned dogs of multiple breeds were recruited by the end of the study, them being: 8 Miniature Schnauzers (20.0%), 6 Miniature poodles (15.0%),4 Mixed-breed (10.0%), 3 Shih-Tzus (7.5%), 3 Pinschers (7.5%), 3 Malteese (7.5%), 3 Yorkshire terriers (7.5%), 3 Lhasa-apso (7.5%), 2 Chihuahuas (5.0%), 2 German Spitz (5.0%), 2 Dachshund (5.0%), and 1 Beagle (2.5%). The age and body weight of the animals ranged from 5-17 years and 2.20-19 kg, respectively. Nineteen, 10, and 11 animals were classified as stages B1, B2 and C, respectively. No difference existed between stages regarding weight ($P= 0.84624$) and age ($P=0.75721$). Demographic data in shown in Table 1.

A significant difference was documented between stages C and B2 from stage B1 patients regarding global circumferential strain. This difference was mainly accounted by the values of regional strain of the middle and basal planes, where a difference was also documented between B1 and C and B1 and B2 patients. A schematic representation of the visual differences in the transversal bulls-eye mapping of stage B1 and stage C patients is shown in Figure 3. Box-plots depicting the differences between groups are show in Figure 4.

Regarding conventional echocardiographic parameters, significant negative

correlations were found between global circumferential strain and the following echocardiographic variables: LA/Ao (ρ = -0.4660), nLVDd (ρ = -0.4291) and Emax (ρ = -0.3840).

DISCUSSION

Global left ventricular contraction depends on properties that are intrinsic to the cardiomyocytes (inotropy), as well as loading conditions of the left ventricle [17]. Assessing systolic function in MMVD dogs has long been a challenge, due to the load-dependent nature of shortening and ejection fraction, conventionally used to determine systolic function in standard echocardiographic studies [7]. To overcome this limitation, strain techniques derived from speckle tracking echocardiography have recently been gaining acceptance in veterinary medicine [11, 12, 13]. In this study, we applied an unconventional imaging method to collect information regarding myocardial mechanics, known as the bulls-eye diagram. Bulls-eye mapping is a tool that gives visual information acquired through 2D image planes that are put together in the form of a target, resulting in a 3D-like experience of left ventricular imaging, where the segments are color-coded according to the degree of myocardial stretch. This gives individual and straightforward information regarding the existence of focal or global deficits in myocardial contraction or synchrony, as wells as allowing the identification of repeatable patterns [18]. In our study, this technique showed segments of impaired myocardial contraction, which resulted in a decrease in left ventricular global circumferential strain, that did not show as impaired FS% and EF% in standard echocardiography. In addition, the results showed that the myocardial regions that are preferably affected consist of the basal and mid regions, with an apparent apical sparing. In medicine, cardiac amyloidosis is known to cause a similar kind of pattern for longitudinal strain, known as “cherry on top”. This infiltrative disease apparently affects the myocardium in this specific pattern, which makes the bulls-eye diagram a helpful tool for early detection of systolic disfunction [11,18].

Previous studies involving speckle tracking derived strain techniques in dogs with MMVD showed and increase in circumferential strain [12]. The conflicting results may be due

to the stage of disease progression in the patients involved in each study, since the previous study did not involve stage C patients.

Left cardiac remodeling and stretching of the myocardial fibers may also lead to the development of arrhythmias especially mediated by anatomical substrate and a disrupted autonomic nervous system [19,20]. The bulls-eye mapping may be a promising tool for the detection of hypokinetic areas due to fibrosis, that might be responsible for arrhythmogenesis, although it was not possible to investigate this feature in this study due to a small number of patients with ventricular arrhythmias. In addition, a repeatable visual pattern of impaired myocardial mechanics was not identified in the animals of study. However, individual identification of focci of decreased left ventricular strain or dysynchrony may account as a useful parameter in follow-up echocardiograms, especially with the detection of arrhythmias in auscultation or electrocardiographic examination. Future studies aiming at this goal may lead to promising results regarding arrhythmia risk stratification.

Finally, the significant negative correlations found between GCS and parameters of cardiac remodeling and increased left ventricular filling pressures supports the hypothesis that circumferential myocardial fibers are affected with disease progression. On the other hand, the lack decreases in conventional echocardiographic parameters of systolic function such as FS% and EF% are in accordance with literature that radial systolic function is only identified in latter stages [8,21]. In severe cases of MR, there is an increase in preload due to volume retention and remodeling, and a decrease in afterload caused by a reduction in peak systolic wall stress [22]. These alterations foster normal to hyperdynamic ventricular contraction, despite impaired myocardial cell contraction, due to the Frank-Starling principle [7]. Thus, conventional echocardiography fails to identify LV systolic dysfunction until it is relatively advanced, and variables that reflect radial contraction can be very misleading [23,24] The results of this study intend to shed a light in myocardial mechanics in these patients, allowing early detection of systolic disfunction, that might someday aid in improved medical therapy and prognosis.

This study has clear limitations, starting from a relatively small sample size, limiting the

identification of repeatable patterns, and well as correlations with ventricular arrhythmias. Also, the strain variables are derived from proprietary algorithms that are not uniform across vendors, which may play a role in the differences between studies [25]. Lastly, good quality images are essential for precise myocardial tracking and, although an effort was made to select only proper samples, the patients in this study were not sedated, resulting in partial loss of quality due to breathing and consious movement.

CONCLUSIONS

The bulls-eye mapping is a contemporary assessment of myocardial mechanics that may clarify systolic function in MMVD dogs. More studies are warranted to discover if specific patterns are indicative of a region of preference in myocardial compromise, as well as its role in identifying arrhythmogenic substrate.

REFERRENCES

1. Keene BW, Atkins CE, Bonagura JD, Fox PR, Haaggstrom J, Fuentes VL, Oyama MA, Rush JE, Stepien R, Uechi M. ACVIM consensus guidelines for the diagnosis and treatment of myxomatous mitral valve disease in dogs. J Vet Intern Med 2019;33:1127e40.

2. Fox, PR. Pathology of myxomatous mitral valve disease in dog. Journal of Veterinary Cardiology, p.103-126, 2012

3. Urabe Y, Mann DL, Kent RL, Nakano K, Tomanek RJ, Carabello BA, Cooper G. Cellular and ventricular contractile dysfunction in experimental canine mitral regurgitation. Circ Res 1992;70:131e147.

4. Kittleson MD, Eyster GE, Knowlen GG, Bari Olivier N, Anderson LK. Myocardial function in small dogs with chronic mitral regurgitation and severe congestive heart failure. J Am Vet Med Assoc 1984;184:455e9.

5. Borgarelli M, Savarino P, Crosara S. Survival characteristics and prognostic variables of dogs with mitral regurgitation attributable to myxomatous valve disease. Journal of Veterinary Internal Medicine, 2008 v.22, p.120-128,
6. Chetboul, V., Tissier, R.. Echocardiographic assessment of canine degenerative mitral valve disease. Journal of Veterinary Cardiology 2012 14, 127-148
7. Bonagura JD, Schober KE. Can ventricular function be assessed by echocardiography in chronic canine mitral valve disease? J Small Anim Pract 2009;50:12e24.
8. Streeter DD, Sportnitz HM. Fiber orientation in the canine left ventricle during diastole and systole. Circ Res 1969;14: 339e47.
9. Sengupta PP, Korinek J, Belohlavek M, Narula J, Vannan MA, Jahangir A, Khandheria BK. Left ventricular structure and function - basic science for cardiac imaging. J Am Coll Cardiol 2006;48:1988e2001.
10. Buss Sj, Mereles D, Emami M, Korosoglou G, Riffel Jh, Bertel D, Schonland So, Hegenbart U, Katus Ha, Hardt Se. Rapid assessment of longitudinal systolic left ventricular function using speckle tracking of the mitral annulus. Clinical Research in Cardiology 2012;101:273e80.
11. Zois NE, Tidholm A, Nagga KM, Moesgaard SG, Rasmussen CE, Ha¨ggstrro¨m J, Pedersen HD, Ablad B, Nilsen HY, Olsen LH. Radial and longitudinal strain and strain rate assessed by speckle-tracking echocardiography in dogs with myxomatous mitral valve disease. J Vet Intern Med 2012;26:1309e19.
12. Smith DN, Bonagura JD, Culwell NM, Schober KE Left ventricular function quantified by myocardial strain imaging in small-breed dogs with chronic mitral regurgitation Journal of Veterinary Cardiology (2012) 14, 231e242
13. Chetboul V, Serres F, Gouni V, Tissier R, Pouchelon JL. Noninvasive assessment of systolic left ventricular torsion by 2-dimensional speckle tracking

imaging in the awake dog: repeatability, reproducibility, and comparison with tissue Doppler imaging variables. J Vet Intern Med 2008;22: 342e350.

14. Nunzio DD, Recupero A, Gregorio C, Zito C, Carerj S, Di Bella G Echocardiographic Findings in Cardiac Amyloidosis: Inside Two-Dimensional, Doppler, and Strain Imaging Current Cardiology Reports (2019) 21:7
15. Liu L, Tuos Z, Zuol L, Haol SY, Shao H, Qi W, Zhou X, Ge S. Reduction of left ventricular longitudinal global and segmental systolic functions in patients with hypertrophic cardiomyopathy: study of two- dimensional tissue motion annular displacement. Exp Ther Med 2014;7:1457e64.
16. Cornell CC, Kittleson MD, Della Torre P, Ha¨ggstro¨m J, Lombard CW, Pedersen HD, Vollmar A, Wey A. Allometric scaling of M-mode cardiac measurements in normal adult dogs. J Vet Intern Med 2004;18:311e21.
17. Atkins CE, Curtis MB, Mcguirk SM, Kittleson MD, Sato T, Snyder PS. The Use of M-Mode Echocardiography in Determining Cardiac output in dogs with normal, low, and high output states: comparison to thermodilution method. Vet Radiol Ultrasound 1992;33:297e304.
18. Phelan D, Collier P, Thavendiranathan P, Popovic Z, Hanna M, Plana JC, Marwick TH, Thomas JD Relative apical sparing of longitudinal strain using two-dimensional speckle-tracking echocardiography is both sensitive and specific for the diagnosis of cardiac amyloidosis Heart 2012;98:1442e1448.
19. Zuppiroli A, Mori F, Favilli S, et al. Arrhythmias in mitral valve prolapse: relation to anterior mitral leaflet thickening, clinical variables, and colour Doppler echocardiographic parameters. Am Heart J 1994; 128: 919–27.

20. Crosara S, Borgarelli M, Haggstrom J. Holter monitoring in 36 dogs with myxomatous mitral valve disease. The Journal of the Australian Veterinary Association, 2010 v. 88, n.10, p.386-391

21. Mizuguchi Y, Oishi Y, Miyoshi H, Iuchi A, Nagase N, Oki T. The functional role of longitudinal, circumferential and radial myocardial deformation for regulating the early impairment of left ventricular contraction and relaxation in patients with cardiovascular risk factors: a study with two-dimensional strain imaging. J Am Soc Echocardiogr 2008;21:1138e44.

22. Katayama K, Tajimi T, Guth BD, Matsuzaki M, Lee JD, Seitelberger R, Peterson KL. Early diastolic filling dynamics during experimental mitral regurgitation in the conscious dog. Circulation 1988;78:390e400.

23. Edvardsen T, Helle-Valle T, Smiseth OA. Systolic dysfunction in heart failure with normal ejection fraction: speckle- tracking echocardiography. Prog Cardiovasc Dis 2006;49: 207e214.

24. McGinley JC, Berretta RM, Chaudhary K, Rossman E, Bratinov GD, Gaughan JP, Houser S, Margulies KB. Impaired contractile reserve in severe mitral valve regurgitation with a preserved ejection fraction. Eur J Heart Fail 2007;9: 857e864.

25. Marwick TH. Consistency of myocardial deformation imaging between vendors. Eur J Echocardiogr 2010;11: 414e416.

TABLES AND FIGURES

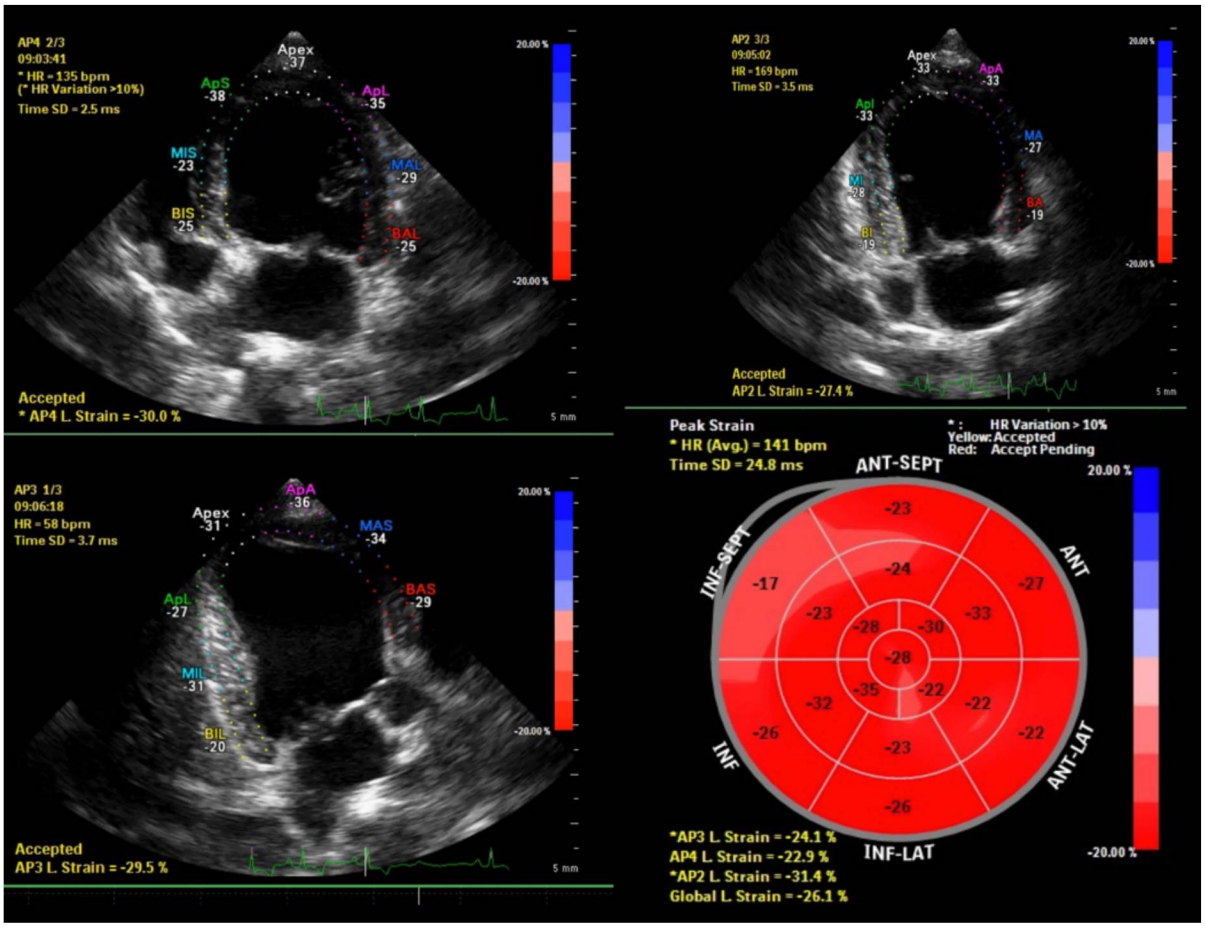

Figure 1
Representation of the automated screening of the 3 longitudinal planes (AP4, AP3 and AP2) and the resulting bull's eye mapping. The longitudinal peek strain of the 18 different myocardial segments is displayed on the same diagram. The value of each global strain for the three different planes is displayed as AP3 L. Strain (-24.1%), AP4 L. Strain (-22.9%) and AP2 L. Strain (-31.4%), along with the resulting Global L. Strain (-26.1%). The homogeneous color coding of the segments indicates, at first glance, longitudinal deformation synchronism, with discrete focal decreased deformation in the septal segment. AP4 apical 4 chambers; AP3 apical 3 chambers; AP2 apical 2 champers; INF-SEPT inferior septal segment; ANT-SEPT anterior septal segment; ANT anterior segment; ANT-LAT anterior lateral segment; INF-LAT inferior lateral segment; INF inferior segment.

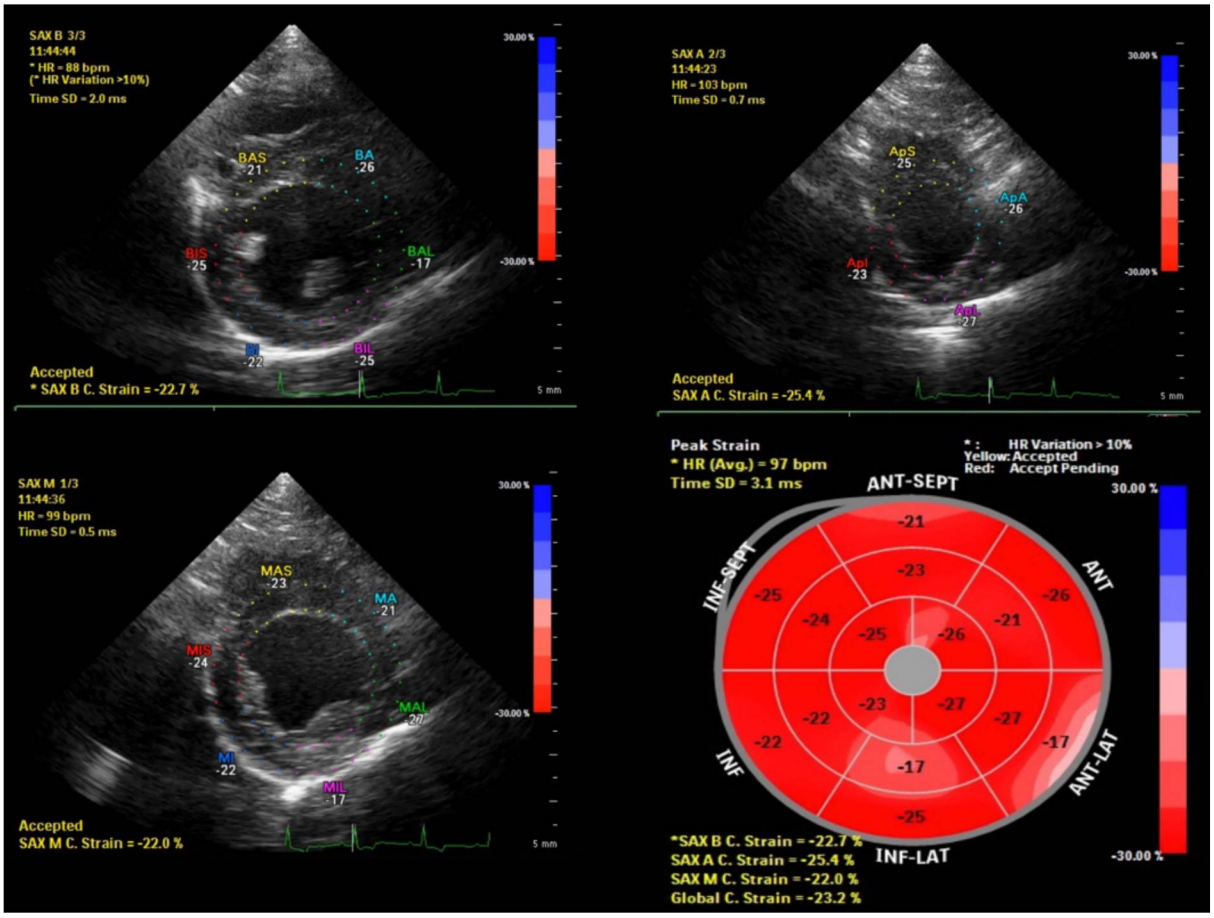

Figure 2
Representation of the automated screening of the 3 transversal planes (SAX B, SAX A, SAX M) and the resulting bull's eye mapping. The circumferential peek strain of the 17 different myocardial segments is displayed on the same diagram. The value of each global strain for the three different planes is displayed as SAX B C. Strain (-22.7%), SAX A C. Strain (-25.4%) and SAX M C. Strain (-22.0%), along with the resulting Global C. Strain (-23.2%). The color coding of the segments indicates circumferential deformation synchronism, with discrete spread out foccis of decreased deformation, especially in the inferior lateral and anterior lateral segments. SAX B transversal basal plane; SAX A transversal apical plane; SAX M transversal mid plane; INF-SEPT inferior septal segment; ANT-SEPT anterior septal segment; ANT anterior segment; ANT-LAT anterior

Table 1. Demographic features of dogs with MMVD.

Variables	Groups						Total		*p**
	B1		B2		C				
	n	%	n	%	n	%	n	%	
Sex									
Male	11	27,5	4	10	7	17,5	22	55	0,52076
Female	8	20	6	15	4	10	18	45	
	Mean±SD								
Age (Years)	12,2±3,34		12,1±3,2		11,4±2,8		11,9±3,10		0,7691
Weight (Kg)	7,2±2,7		5,4±1,8		7,0±4,9		6,7±3,3		0,3764

Results of age and weight are presented as mean ± standard deviation. MMVD myxomatous mitral valve disease; SD standard deviation.

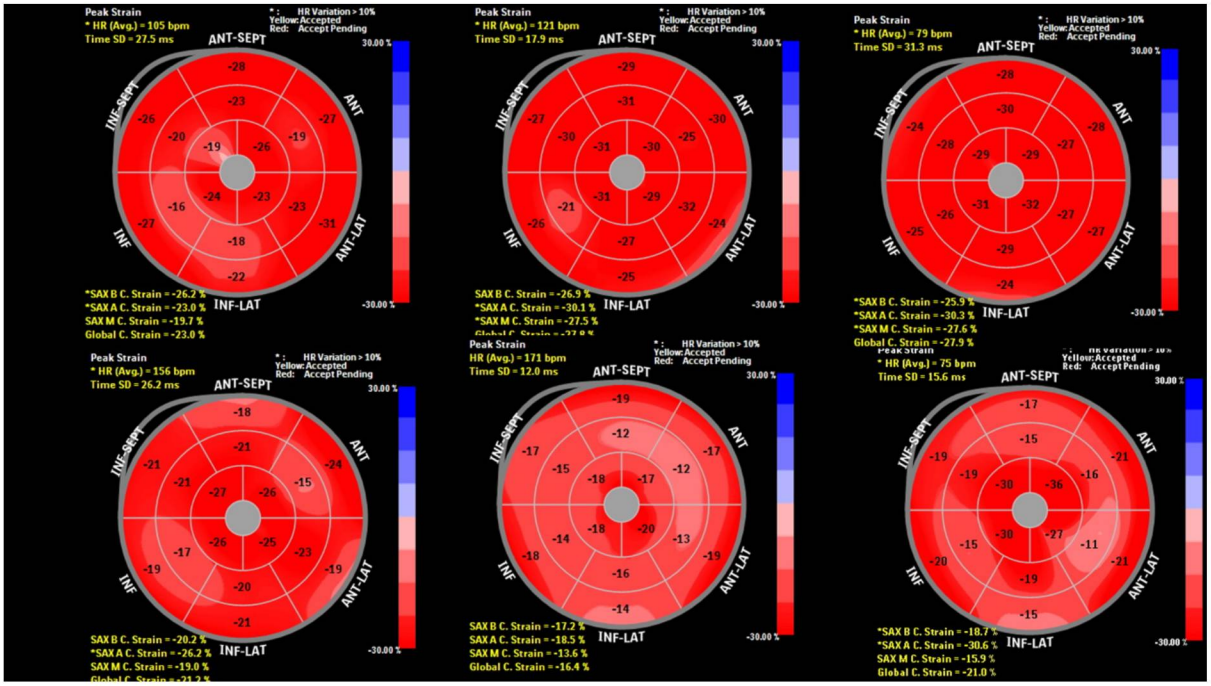

Figure 3. Representation of the resulting transversal bull's eye mapping of three stage B1 patients (upper row) and 3 stage C patients (lower row). The uniform color coding in the upper row indicates synchrony and preserved circunferentical deformation of the segments. The nonuniform color coding in the lower row indicates circumferential deformation desynchrony, with spread out foccis of decreased circumferential contraction of the fibers, especially in the inferior lateral and anterior lateral segments.

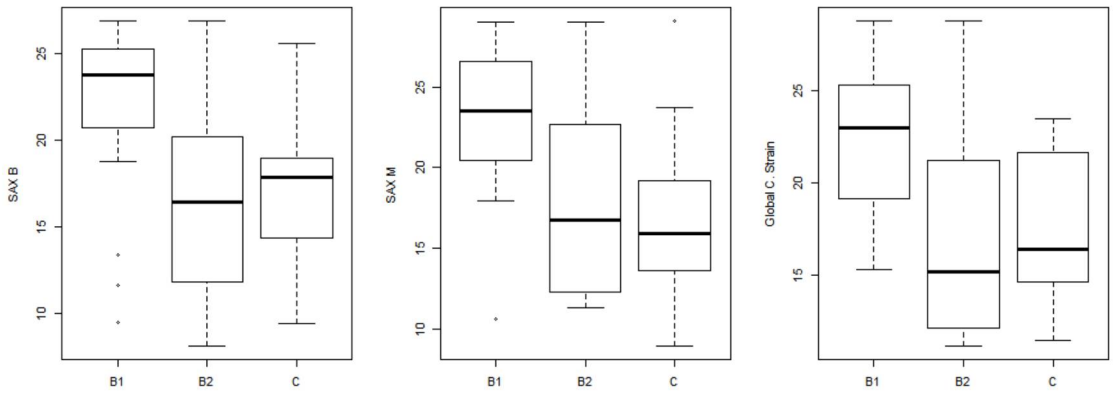

Figure 4. Box plots depicting the medians, interquartile ranges, and amplitude of SAX B circumferential strain, SAX M circumferential strain and Global Circumferential strain in dogs in different stages of myxomatous mitral valve disease. Outliers are shown. SAX B transversal basal plane; SAX M transversal mid plane, Global C Strain.

REFERÊNCIAS

ATKINS, C.; BONAGURA, J.; ETTINGER, S.; FOX, P.; GORDON, S.; HAGGSTROM, J.; HAMLIN, R.;KEENE, B.; LUIS-FUENTES, V.; STEPIEN, R. Guidelines for the diagnosis and treatment of canine chronic valvular heart disease. **Journal of Veterinary Internal Medicine**, v.23, n.6, p.1142-1150, 2009.

ATKINS CE, CURTIS MB, MCGUIRK SM, KITTLESON MD, SATO T, SNYDER PS. The Use of M-Mode Echocardiography in Determining Cardiac output in dogs with normal, low, and high output states: comparison to thermodilution method. **Vet Radiol Ultrasound** 1992;33:297e304.

BAAD M, LU ZF, REISER I, ET AL. Clinical significance of US artifacts. **Radiographics** 2017:37;1408–1423.

BARR CS, NAAS A, FREEMAN M, LANG CC, STRUTHERS AD. QT dispersion and sudden unexpected death in chronic heart failure. **Lancet** 1994;343:327e9.

BALBARINI A, LIMBRUNO U, BERTOLI D, et al. Evaluation of pulmonary vascular pressures in cardiac patients: The role of the chest roentgenogram. **J Thorac Imaging** 1991:6;62–68.

BERGER R, KASPER E, BAUGHMAN K, MARBAN E, CALKINS H, & TOMASELLI G. Beat-to- beat QT interval variability. Novel evidence for repolarization lability in ischemic and nonischemic dilated cardiomyopathy. **Circulation**, 1997 96, 1557– 1565.

BONAGURA, J.D.; SCHOBER, K.E. Can ventricular function be assessed by echocardiography in chronic canine mitral valve disease? **Journal of Small Animal Practice**, v.50, supll.1, p.12-24, 2009.

BORGARELLI, M.; HAGGSTROM, J. Canine Degenerative myxomatous mitral valve disease: natural history, clinical presentation and therapy. **Vet Clin Small Anim** v.40, p.651–663, 2010

BORGARELLI, M., SAVARINO, P., CROSARA, S. Survival characteristics and prognostic variables of dogs with mitral regurgitation attributable to myxomatous valve disease. **Journal of Veterinary Internal Medicine** 22: 120–128, 2008

BORGARELLI, M.; ZINI, E.; D'AGNOLO, G.; et al. Comparison of primary mitral valve disease in German shepherd dogs and in small breeds. **Journal of Veterinary Cardiology.** v.6:27-34, 2004.

BORLEFFS CJ, SCHERPTONG RW, MAN SC, et al. Predicting ventricular arrhythmias in patients with ischemic heart disease: clinical application of the ECG-derived QRS-T angle. **Circ Arrhythm Electrophysiol** 2009;2:548–554.

BUSS SJ, MERELES D, EMAMI M, KOROSOGLOU G, RIFFEL JH, BERTEL D, SCHONLAND SO, HEGENBART U, KATUS HA, HARDT SE. Rapid assessment of longitudinal systolic left ventricular function using speckle tracking of the mitral annulus. **Clinical Research in Cardiology** 2012;101:273e80.

BRÜLER, BC.; JOJIMA, FS.; DITTRICH, G.; GIANNICO, AT.; SOUSA, MG. QT instability, an indicator of augmented arrhythmo- genesis, increases with the

progression of myxomatous mitral valve disease in dogs. **Journal of Veterinary Cardiology v**.66 p254-66, 2018.

CHEN, X.; TERESHCHENKO, L.G.; BERGER, R.D.; TRAYANOVA, N.A.; Arrhythmia Risk Stratification based on QT Interval Instability: An Intracardiac Electrocardiogram Study, **Heart Rhythm**, v.10, n.6, p.875–880, 2013

CHETBOUL V, SERRES F, GOUNI V, TISSIER R, POUCHELON JL. Noninvasive assessment of systolic left ventricular torsion by 2-dimensional speckle tracking imaging in the awake dog: repeatability, reproducibility, and comparison with tissue Doppler imaging variables. **J Vet Intern Med** 2008;22: 342e350.

CHETBOUL V, TISSIER R. Echocardiographic assessment of canine degenerative mitral valve disease. **Journal of Veterinary Cardiology** 2012:14;127-148.

CHUA KCM, TEODORESCU C, REINIER K, et al. Wide QRST angle on the 12-Lead ECG as a predictor of sudden death beyond the LV ejection fraction. **J Cardiovasc Electrophysiol**. 2016;27:833-839.

CORNELL CC, KITTLESON MD, DELLA TORRE P, et al. Allometric scaling of M-mode cardiac measurements in normal adult dogs. **J Vet Intern Med** 2004;18:311–321.

CROSARA, S.; BORGARELLI, M.; HAGGSTROM, J. Holter monitoring in 36 dogs with myxomatous mitral valve disease. **The Journal of the Australian Veterinary Association**, v. 88, n.10, p.386-391, 2010

DEAR JD. Bacterial Pneumonia in Dogs and Cats: An Update. **Vet Clin North Am Small Anim Pract**. 2020:50(2);447-465.

DIANA A, GUGLIELMINI C, PIVETTA M, et al. Radiographic features of cardiogenic pulmonary edema in dogs with mitral regurgitation: 61 cases (1998–2007). **J Am Vet Med Assoc** 2009:235;1058–1063.

EDVARDSEN T, HELLE-VALLE T, SMISETH OA. Systolic dysfunction in heart failure with normal ejection fraction: speckle- tracking echocardiography. **Prog Cardiovasc Dis** 2006;49: 207e214.

FEISSEL M, MAIZEL J, ROBLES G, et al. Clinical relevance of echocardiography in acute severe dyspnea. **J Am Soc Echocardiogr** 2009:22;1159–1164.

FINE DM, DECLUE AE, REINERO CR. Evaluation of circulating amino terminal-pro-B-type natriuretic peptide concentration in dogs with respiratory distress attributable to congestive heart failure or primary pulmonary disease. **J Am Vet Med Assoc** 2008:232;1674–1679.

FOX, PR. Pathology of myxomatous mitral valve disease in dog. **Journal of Veterinary Cardiology**, p.103-126, 2012

GÜNER A, KALÇIK M, ÇELIK M, et al., Impaired repolarization parameters may predict fatal ventricular arrhythmias in patients with hypertrophic cardiomyopathy (from the CILICIA Registry), **Journal of Electrocardiology** (2020), https://doi.org/10.1016/j.jelectrocard.2020.10.009

HAGGSTROM, J.; HOGLUNG, K.; BORGARELLI, M. An update on treatment and prognostic indicators in canine myxomatous mitral valve disease. **Journal of Small Animal Practice**, v.50 p.25-33, 2009

HAIGNEY MC, WEI S, KAAB S, et al. Loss of cardiac magnesium in experimental heart failure prolongs and destabilizes repolarization in dogs. **J Am Coll Cardiol**. 1998 31:701–706.

HANSSON K, HAGGSTROM J, KVART C, LORD P. Left atrial to aortic root indices using two-dimensional and M-mode echocardiography in cavalier King Charles spaniels with and without left atrial enlargement. **Vet Radiol Ultrasound.** 2002:43(6);568-575.

HORI Y, YAMASHITA Y, SAKAKIBARA K, et al. Usefulness of pericardial lung ultrasonography for the diagnosis of cardiogenic pulmonary edema in dogs. **Am J Vet Res** 2020:81;227-232.

JOHNSON EG, WISNER ER. Advances in respiratory imaging. **Vet Clin North Am Small Anim Pract**. 2007:37(5);879-900.

KATAYAMA K, TAJIMI T, GUTH BD, MATSUZAKI M, LEE JD, SEITELBERGER R, PETERSON KL. Early diastolic filling dynamics during experimental mitral regurgitation in the conscious dog. **Circulation** 1988;78:390e400.

KEENE, BW.; ATKINS, CE.; BONAGURA, JD.; FOX ,PR.; HAÄGGSTROM, J.; FUENTES, VL.; OYAMA, MA.; RUSH, JE.; STEPIEN, R.; UECHI, M. ACVIM consensus guidelines for the diagnosis and treatment of myxomatous mitral valve disease in dogs. **Journal of Veterinary Internal Medicine** v. 33 p1127-40, 2019

KITTLESON MD, EYSTER GE, KNOWLEN GG, BARI OLIVIER N, ANDERSON LK. Myocardial function in small dogs with chronic mitral regurgitation and severe congestive heart failure. **J Am Vet Med Assoc** 1984;184:455e9.

LABOVITZ AJ, NOBLE VE, BEIRIG M, et al. Focused cardiac ultrasound in the emergent setting: a consensus statement of the American Society of Echocardiography and American College of Emergency Physicians. **J Am Soc Echocardiogr** 2010;23:1225–30.

LICHTENSTEIN D, MEZIERE G, BIDERMAN P, et al. The comet-tail artifact. An ultrasound sign of alveolar-interstitial syndrome. **Am J Respir Crit Care Med** 1997:156;1640–1646.

LISCIANDRO GR, FOSGATE GT, FULTON RM. Frequency and number of ultrasound lung rockets (B-lines) using a regionally based lung ultra- sound examination named vet BLUE (veterinary bedside lung ultra- sound exam) in dogs with radiographically normal lung findings. **Vet Radiol Ultrasound** 2014:55;315-322.

LISCIANDRO GR, FULTON RM, FOSGATE GT, et al. Frequency of B-lines using a regionally-based lung ultrasound examination in cats with normal thoracic radiographically normal lungs compared with left- sided congestive heart failure. **J Vet Emerg Crit Care** 2017: 27(5);499– 505.

LIU, L.;TUOS,ZHANGJ,ZUOL,LIUF,HAOL,SUNY,YANGL, SHAO H, QI W, ZHOU X, GE S. Reduction of left ventricular longitudinal global and segmental systolic functions in patients with hypertrophic cardiomyopathy: study of two- dimensional tissue motion annular displacement. **Exp Ther Med** 2014;7:1457e64.

LOUVET A, BOURGEOIS JM. Lung ring-down artifact as a sign of pulmonary alveolar-interstitial disease. **Vet Radiol Ultrasound** 2008:49;374–377

MARTINDALEJ L,WAKAI A,COLLINS SP, et al.Diagnosing acute heart failure in the emergency department: a systematic review and meta-analysis. **Acad Emerg Med**. 2016:23;223-242.

MARWICK TH. Consistency of myocardial deformation imaging between vendors. **Eur J Echocardiogr** 2010;11: 414e416.

MASSEAU I, REINERO CR. Thoracic computed tomographic interpretation for clinicians to aid in the diagnosis of dogs and cats with respiratory disease. **Veterinary Journal.** 2019:253;1053-88.

MCGINLEY JC, BERRETTA RM, CHAUDHARY K, ROSSMAN E, BRATINOV GD, GAUGHAN JP, HOUSER S, MARGULIES KB. Impaired contractile reserve in severe mitral valve regurgitation with a preserved ejection fraction. **Eur J Heart Fail** 2007;9: 857e864.

MEURS, KM.; FRIEDENBERG, SG.; WILLIAMS, B, et al. Evaluation of genes associated with human myxomatous mitral valve disease in dogs with familial myxomatous mitral valve degeneration. **Vet J.** v.232 p.16-19, 2018.

MIZUGUCHI Y, OISHI Y, MIYOSHI H, IUCHI A, NAGASE N, OKI T. The functional role of longitudinal, circumferential and radial myocardial deformation for regulating the early impairment of left ventricular contraction and relaxation in patients with cardiovascular risk factors: a study with two-dimensional strain imaging. **Journal of the American Society of Echocardiography** 2008;21:1138e44.

NUNZIO DD, RECUPERO A, GREGORIO C, ZITO C, CARERJ S, DI BELLA G Echocardiographic Findings in Cardiac Amyloidosis: Inside Two-Dimensional, Doppler, and Strain Imaging **Current Cardiology Reports** (2019) 21:7

OEHLER A, FELDMAN T, HENRIKSON C, TERESHCHENKO L. QRS-T Angle: A Review. **Ann Noninvasive Electrocardiol** 2014;19(6):534–542.

OHNO M, CHENG CP, LITTLE WC. Mechanism of altered patterns of left ventricular filling during the development of congestive heart failure. **Circulation** 1994:89;2241–2250

OLSEN TF, ALLEN AL. Causes of sudden and unexpected death in dogs: a 10-year retrospective study. **Can Vet J** 2000;41:873e5.

OYAMA MA, FOX PR, RUSH JE, et al. Clinical utility of serum N-terminal pro-B-type natriuretic peptide concentration for identifying cardiac disease in dogs and assessing disease severity. **J Am Vet Med Assoc** 2008:232;1496–1503

THOMSEN B, TRUIN M, OPSTAL JM, BEEKMAN JD, VOLDERS PG, STENGL M, VOS MA. Sudden cardiac death in dogs with remodeled hearts is associated with larger beat-to-beat variability of repolarization. **Basic Res Cardiol** 2005;100: 279e87.

PALANISWAMY C, SINGH T, ARONOW WS, et al. A planar QRS-T angle> 90 degrees is associated with multivessel coronary artery disease in patients undergoing coronary angiography. **Med Sci Monit**. 2009;15: MS31-MS34.

PHELAN, D.; COLLIER, P.;THAVENDIRANATHAN, P; et al. Relative apical sparing of longitudinal strain using two-dimensional speckle-tracking echocardiography is both sensitive and specific for the diagnosis of cardiac amyloidosis. **Heart** v. 98 p1442-1448, 2012.

RADEMACHER N, PARIAUT R, PATE J, et al. Transthoracic lung ultrasound in normal dogs and dogs with cardiogenic pulmonary edema: A pilot study. **Vet Radiol Ultrasound** 2014; 55;447–452.

RAMÍREZ, E.Y.; PLALANCA, I. M. Manejo de la insuficiencia cardíaca congestiva In: BELENERIAN, G.C.; MUCHA, C.J; CAMACHO, A.A. **Afecciones cardiovasculares em pequeños animales**. 1. ed. Buenos Aires: Intermédica, 2001

REYNOLDS CA, BROWN DC, RUSH JE Prediction of first onset of congestive heart failure in dogs with degenerative mitral valve disease: the PREDICT cohort study. **Journal of Veterinary Cardiology** 2012; 14, 193-202

ROZANSKI E, CHAN D. Approach to the patient with respiratory distress. **Vet Clin North Am Small Anim Pract** 2005;35(2):307-317.

SANTILLI, RA; (2018). Chapter 2: Principals of Electrocardiography. In Santilli, Ra.; Moïse, S.; Pariaut, R.; Perego, M, **Electrocardiography of the Dog and Cat** (2ª ed., pp. 21-65). Edra S.p.A.

SENGUPTA PP, KORINEK J, BELOHLAVEK M, NARULA J, VANNAN MA, JAHANGIR A, KHANDHERIA BK. Left ventricular structure and function - basic science for cardiac imaging. **J Am Coll Cardiol** 2006;48:1988e2001.

SCHOBER KE, BONAGURA JD, SCANSEN BA, et al. Estimation of left ventricular filling pressure by use of Doppler echocardiography in healthy anesthetized dogs subjected to acute volume loading. **Am J Vet Res** 2008:69;1034–1049.

SCHOBER KE, HART TM, STERN JA, et al. Detection of congestive heart failure in dogs by Doppler echocardiography. **J Vet Intern Med** 2010:24;1358-1368.

SMITH DN, BONAGURA JD, CULWELL NM, SCHOBER KE Left ventricular function quantified by myocardial strain imaging in small-breed dogs with chronic mitral regurgitation **Journal of Veterinary Cardiology** (2012) 14, 231e242

STREETER DD, SPORTNITZ HM. Fiber orientation in the canine left ventricle during diastole and systole. **Circ Res** 1969;14: 339e47.

TSE YC, RUSH JE, CUNNINGHAM SM, et al. Evaluation of a training course in focused echocardiography for noncardiology house officers. **J Vet Emerg Crit Care.** 2013: 23(3);268-73.

URABE Y, MANN DL, KENT RL, NAKANO K, TOMANEK RJ, CARABELLO BA, COOPER G. Cellular and ventricular contractile dysfunction in experimental canine mitral regurgitation. **Circ Res** 1992;70:131e147.

VERHEULE, S.; WILSON, E.; EVERETT, T.; SHANBHAG, S.; GOLDEN, C.; OLGIN, J. Alterations in atrial electrophysiology and tissue structure in a canine model of chronic atrial dilatation due to mitral regurgitation. **Circulation**, v.107, p.2615-2622, 2003.

VILA, BC.; CAMACHO, AA,; SOUSA, MG. T-wave peak-end interval and ratio of T-wave peak-end and QT intervals: novel arrhythmogenic and survival markers for dogs with myxomatous mitral valve disease. **Journal of Veterinary Cardiology** v.35, 25-41, 2021

WARD JL, LISCIANDRO GR, DEFRANCESCO TC. Distribution of alveolar-interstitial syndrome in dogs and cats with respiratory distress as assessed by lung ultrasound versus thoracic radiographs. **J Vet Emerg Crit Care** (San Antonio) 2018:28;415–428.

WARD JL, LISCIANDRO GR, KEENE BW, et al. Accuracy of point-of-care lung ultrasonography for the diagnosis of cardiogenic pulmonary edema in dogs and cats with acute dyspnea. **J Am Vet Med Assoc**. 2017:250;666-675.

WARE, W. A. O exame cardiovascular. In: NELSON, R. W.; COUTO, C. G. (Ed.) **Medicina interna de pequenos animais**. 2. ed. Rio de Janeiro

WHITNEY, J.C. Observation on the effect of age in the severity of heart valve lesions in the dog. **Journal of Small Animal Practice**, v.15, n.8, p.511-522, 1974.

ZOIS, NE., TIDHOLM, A., NAGGA, KM., MOESGAARD, SG., RASMUSSEN, CE., HA ÄGGSTRROM, J.; PEDERSEN, HD.; ABLAD, B.; NILSEN, HY.; OLSEN, LH. Radial and longitudinal strain and strain rate assessed by speckle-tracking echocardiography in dogs with myxomatous mitral valve disease. **Journal of Veterinary Internal Medicine** v.26 1309-19, 2012.

ZUPPIROLI A, MORI F, FAVILLI S, et al. Arrhythmias in mitral valve prolapse: relation to anterior mitral leaflet thickening, clinical variables, and colour Doppler echocardiographic parameters. **Am Heart J** 1994; 128: 919–27.

ANEXO - Aprovação pelo Comitê de Ética do Setor de Ciências Agrárias da Universidade Federal do Paraná

UNIVERSIDADE FEDERAL DO PARANÁ SETOR DE CIÊNCIAS AGRÁRIAS COMISSÃO DE ÉTICA NO USO DE ANIMAIS

CERTIFICADO

Certificamos que o protocolo número 094/2018, referente ao projeto **"Relação entre função sistólica multidirecional, morfologia valvar mitral e arritmogênese ventricular em cães com degeneração mixomatosa da valva mitral",** sob a responsabilidade **Marlos Gonçalves Sousa** – que envolve a produção, manutenção e/ou utilização de animais pertencentes ao filo Chordata, subfilo Vertebrata (exceto o homem), para fins de pesquisa científica ou ensino – encontra-se de acordo com os preceitos da Lei no 11.794, de 8 de Outubro, de 2008, do Decreto no 6.899, de 15 de julho de 2009, e com as normas editadas pelo Conselho Nacional de Controle da Experimentação Animal (CONCEA), e foi aprovado pela COMISSÃO DE ÉTICA NO USO DE ANIMAIS (CEUA) DO SETOR DE CIÊNCIAS AGRÁRIAS DA UNIVERSIDADE FEDERAL DO PARANÁ - BRASIL, com grau 2 de invasividade, em reunião de 05/12/2018.

Vigência do projeto	Janeiro/2019 até Janeiro/2022
Espécie/Linhagem	*Canis familiaris* (cão)
Número de animais	300
Peso/Idade	≤ 15 kg/Variável
Sexo	Macho e fêmea
Origem	Hospital Veterinário da Universidade Federal do Paraná, Curitiba, Paraná, Brasil

CERTIFICATE

We certify that the protocol number 094/2018, regarding the project **"Relationship between multidirectional systolic function, mitral valve morphology andventricular arrhythmogenesis in dogs with myxomatous mitral valve disease"** under **Marlos Gonçalves Sousa** supervision – which includes the production, maintenance and/or utilization of animals from Chordata phylum, Vertebrata subphylum (except Humans), for scientific or teaching purposes – is in accordance with the precepts of Law no 11.794, of 8 October, 2008, of Decree no 6.899, of 15 July, 2009, and with the edited rules from Conselho Nacional de Controle da Experimentação Animal (CONCEA), and it was approved by the ANIMAL USE ETHICS COMMITTEE OF THE AGRICULTURAL SCIENCES CAMPUS OF THE UNIVERSIDADE FEDERAL DO PARANÁ (Federal University of the State of Paraná, Brazil), with degree 2 of invasiveness, in session of 05/12/2018.

Duration of the project	January/2019 until January/2022
Specie/Line	*Canis familiaris* (cão)
Number of animals	300
Wheight/Age	≤ 15 kg/Variable
Sex	Male and Female
Origin	Veterinary Hospital of Federal University of Paraná, Curitiba, Brasil

Curitiba, 05 de dezembro de 2018

Chayani da Rocha

Comissão de Ética no Uso de Animais do Setor de Ciências Agrárias - UFPR